Air-sea CO_2 fluxes along the coast of Chile: From CO_2 outgassing in central northern upwelling waters to CO_2 uptake in southern Patagonian fjords

Rodrigo Torres,[1] Silvio Pantoja,[2,3] Naomi Harada,[4] Humberto E. González,[1,3,5] Giovanni Daneri,[1,3] Máximo Frangopulos,[6,7] José A. Rutllant,[8,9] Carlos M. Duarte,[10,11] Sergio Rúiz-Halpern,[10,11] Eva Mayol,[11] and Masao Fukasawa[4]

Received 16 April 2010; revised 17 June 2011; accepted 14 July 2011; published 9 September 2011.

[1] Carbon system parameters measured during several expeditions along the coast of Chile (23°S–56°S) have been used to show the main spatial and temporal trends of air-sea CO_2 fluxes in the coastal waters of the eastern South Pacific. Chilean coastal waters are characterized by strong pCO_2 gradients between the atmosphere and the surface water, with high spatial and temporal variability. On average, the direction of the carbon flux changes from CO_2 outgassing at the coastal upwelling region to CO_2 sequestering at the nonupwelling fjord region in Chilean Patagonia. Estimations of surface water pCO_2 along the Patagonian fjord region showed that, while minimum pCO_2 levels (strong CO_2 undersaturation) occurs during the spring and summer period, maximum levels (including CO_2 supersaturation) occur during the austral winter. CO_2 uptake in the Patagonia fjord region during spring-summer is within the order of −5 mol C m^{-2} yr^{-1}, indicating a significant regional sink of atmospheric CO_2 during that season. We suggest that the CO_2 sink at Patagonia most probably exceeds the CO_2 source exerted by the coastal upwelling system off central northern Chile.

Citation: Torres, R., et al. (2011), Air-sea CO_2 fluxes along the coast of Chile: From CO_2 outgassing in central northern upwelling waters to CO_2 uptake in southern Patagonian fjords, *J. Geophys. Res.*, *116*, C09006, doi:10.1029/2010JC006344.

1. Introduction

[2] The coastal ocean is characterized by intense biogeochemical cycling forced by the interaction between ocean, land, and atmosphere. The nature of these interactions depends on several factors (e.g., land morphology, ocean and atmosphere circulation patterns, among others) but is generally characterized by large and variable exchanges of matter and energy (e.g., heat, CO_2, water) at the interfaces (e.g., air-sea, sea-sediment).

[3] Carbon exchange at the air-sea interface in coastal areas may play an important role in the global carbon cycle [*Chen and Borges*, 2009]. However, coastal waters have been poorly covered by surveys of air-sea exchange given their high spatial and temporal heterogeneity [*Ducklow and McCallister*, 2004; *Chen and Borges*, 2009]. In coastal zones in the Northern Hemisphere, various researchers have observed that, while high-latitude systems tend to be sinks for atmospheric CO_2, low-latitude systems tend to be sources of CO_2 to the atmosphere [*Borges et al.*, 2005; *Cai et al.*, 2006; *Chavez et al.*, 2007; *Chen and Borges*, 2009]. A global analysis *Takahashi et al.* [2009] showed that this coastal pattern is applicable throughout most of the South Pacific Ocean (~0°S–55°S). However, the resolution and empirical basis for this pattern are very limited in the southeastern Pacific coastal area [*Takahashi et al.*, 2009], in particular, in the large region of fjords and channels of Patagonia. On the basis of a compilation of available measurements of carbonate system parameters, we describe the direction of coastal CO_2 air-sea fluxes off the west coast of South America from the subtropics to high latitudes (23°S–56°S) and discuss the processes and factors that may control these patterns.

[1]Centro de Investigación en Ecosistemas de la Patagonia, Universidad Austral de Chile, Coyhaique, Chile.
[2]Departamento de Oceanografía, Universidad de Concepción, Concepción, Chile.
[3]Centro de Investigación Oceanográfica en el Pacífico Sur Oriental, Universidad de Concepción, Concepción, Chile.
[4]Research Institute for Global Change, Japan Agency for Marine-Earth Science and Technology Center, Yokosuka, Japan.
[5]Instituto de Biología Marina, Universidad Austral de Chile, Valdivia, Chile.
[6]Centro de Estudios del Cuaternario de Fuego-Patagonia, Punta Arenas, Chile.
[7]Universidad de Magallanes, Punta Arenas, Chile.
[8]Departamento de Geofísica, Facultad de Ciencias Físicas y Matemáticas, Universidad de Chile, Santiago, Chile.
[9]Centro de Estudios Avanzados en Zonas Aridas, La Serena, Chile.
[10]Department of Global Change Research, IMEDEA, Instituto Mediterráneo de Estudios Avanzados, Esporles, Mallorca, Spain.
[11]Laboratorio Internacional de Cambio Global, CSIC-PUC, Facultad de Ciencias Biológicas, Pontificia Universidad Católica de Chile, Santiago, Chile.

0148-0227/11/2010JC006344

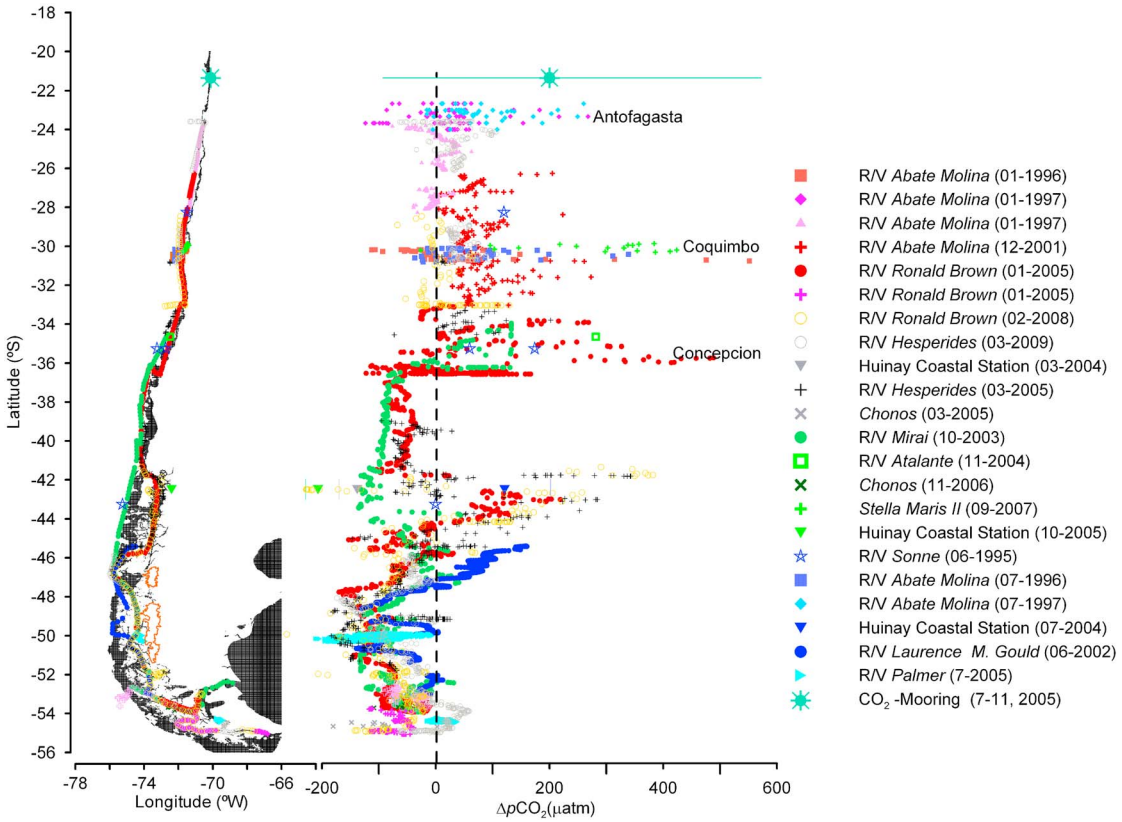

Figure 1. The air-surface water CO_2 gradient (ΔpCO_2) off the Chilean coast. (left) The continental shelf (0–200 m depth) depicted by the black area and the sampling locations depicted by colored symbols. (right) ΔpCO_2 estimated during each expedition, color triangles with associated error bars depict 8–10 day averages and standard deviations of daily observations in the Comau fjord (Huinay Marine Station). ΔpCO_2 mean values of a mooring at 21°S [*Friederich et al.*, 2008] are depicted by a symbol and the corresponding bars represent the range of ΔpCO_2 during the sampling period (see Table 1). The area enclosed by an orange line depicts Northern and Southern Ice Field.

1.1. Study Area, Wind Regimen, and Precipitation Patterns

[4] Contrasting with the straight, smooth, and meridionally oriented coastal line along northern and central Chile (~18°S–40°S), a complex system of fjords and islands extends south of 42°S (Figure 1). Broadly speaking, the axis of the mean position of the west wind belt (~43°S) separates both zones. As we progress equatorward (northward), an increasing influence of the subtropical anticyclone results in upwelling-favorable southerly winds and a decreasing seasonality. The poleward (southward) zone is year-round under the influence of traveling disturbances in the westerlies (cyclones, anticyclones, and associated frontal systems) that result in prevailing northerly (downwelling favorable) winds along the coast [e.g., *Strub et al.*, 1998; *Pizarro*, 2000].

[5] Beyond the low-frequency variability in the strength and position of these climate factors (i.e., subtropical anticyclone, west wind belt, subpolar low) in connection with the Pacific Decadal Oscillation (interdecadal) and El Niño–Southern Oscillation (interannual) cycles, seasonal changes modulate the mean intensity of upwelling-favorable winds along the northern zone. In the northernmost section, upwelling is almost permanent, in particular, during austral spring and summer when coastal winds are stronger in connection with the strong subtropical anticyclone (spring) and the strong land-sea thermal contrast due to the seasonal minimum in low cloud cover (summer). Upwelling here concentrates near the coast because of an anticyclonic windstress curl caused by seasonally weaker trade winds off the coast. In addition, this coastal area is highly sensitive to intraseasonal, equatorially forced, coastally trapped waves that propagate poleward and Rossby waves directed offshore that periodically change the depth of the nutricline/thermocline, which in turn affects the efficiency with which local winds drive upwelling. Mostly south of 27°S, the passage of synoptic-scale disturbances and associated upper-air waves in the west wind belt generate poleward-propagating coastal lows [e.g., *Garreaud et al.*, 2002] that force quasi-weekly strengthening–relaxation cycles in the upwelling-favorable winds. Between 30°S and 35°S, offshore surface winds also peak during the strengthening phase of coastal winds in the form of a jet whose axis is located at about 150–200 km offshore [*Garreaud and Munoz*, 2005]. Therefore, a widening of the coastal upwelling zone associated with the

Ekman drift derives from the cyclonic wind stress curl onshore of the jet axis. This is an almost year-round phenomenon at 30°S, with increasing seasonality southward, appearing only in late spring-summer at 36°S–38°S.

[6] South of 40°S–42°S, synoptic-scale disturbances in the west wind belt are characterized by eastward-drifting cyclones and anticyclones with associated frontal systems, resulting in shifting wind directions superimposed on the prevailing northerlies.

[7] In terms of freshwater input to the coastal ocean, there exists an extreme latitudinal gradient in precipitation, ranging from a negligible mean accumulation per year at Antofagasta (23°S) to more than 7 m at about 50°S (near Guarello Island [*Devynck*, 1971]). In Patagonia, this orographic effect of the Andes Mountains on precipitation is characterized by decreasing mean annual precipitation from about 5000 mm along the coast of western Patagonia to less than 400 mm in the other side of the mountains.

1.2. CO_2 Outgassing in Coastal Upwelling Areas Off Central and Northern Chile

[8] The equatorward, alongshore coastal winds promote upwelling of cold, oxygen-poor water enriched in dissolved inorganic carbon (DIC) and supersaturated in CO_2 [*Torres et al.*, 1999, 2002, 2003; *Torres*, 2001, *Friederich et al.*, 2008, *Paulmier et al.*, 2008; *Goyet et al.*, 2009; *Torres and Ampuero*, 2009]. The immediate CO_2 outgassing caused by upwelling can be enhanced because of the rapid heating of surface waters at these warm latitudes [*Torres et al.*, 1999]. Because the winds that promote upwelling of CO_2-rich waters are also the key factor driving the ventilation of CO_2, the effect of wind stress on CO_2 outgassing is expected to be synergic in upwelling areas off Chile [*Torres et al.*, 1999]. Strong across-shore CO_2 gradients have been reported during active upwelling, with maximum surface water CO_2 supersaturation at the "upwelling foci" (denser surface waters) located closer to the coast [*Torres et al.*, 1999, 2002; *Goyet et al.*, 2009]. Offshore from the introduction belt (i.e., offshore from the region where isopycnals are tilted up with Rossby internal deformation radii of 35–40 km for northern Chile), surface water pCO_2 values are substantially lower and nearer to atmospheric equilibrium [cf. *Torres et al.*, 2002]. The pCO_2 of this offshore water appears to be primarily determined by temperature, because CO_2 supersaturation increases with sea surface temperature (SST) in the salty and oligotrophic subtropical water [*Torres et al.*, 2002]. Meanwhile, filaments of relatively low-salinity waters that propagate offshore from the upwelling foci are slightly undersaturated in CO_2 and exhibit high fluorescence [*Torres*, 2001; *Lefèvre et al.*, 2002], suggesting an active biological pump.

[9] Middepth waters (equatorial subsurface water; ESSW) that feed the deep upwelling off Chile flow into the Peru-Chile undercurrent [*Brandhorst*, 1971; *Silva and Neshyba*, 1979], transporting products of both aerobic (e.g., dissolved oxygen deficit and excess CO_2) and anaerobic (e.g., nitrate deficit and corresponding excess CO_2) respiration from lower to higher latitudes [*Dugdale et al.*, 1977; *Fedele*, 1993; *Fuenzalida et al.*, 2009; *Silva et al.*, 2009]. The upward transport of the nitrate deficit and its associated CO_2 excess (from anaerobic respiration) implies a reduction in the new production when this water returns to the euphotic zone [*Torres*, 2001]. This constraint for new production and concomitant enrichment in CO_2 is one factor that explains the high CO_2 outgassing in waters off northern and central Chile [*Torres*, 2001] and Peru [*Friederich et al.*, 2008].

[10] Above the Chile-Peru undercurrent, a low salinity and more oxygenated subantarctic water mass is advected equatorward from rainy latitudes. This subantarctic water sinks at about 35°S, constituting the shallow salinity minimum that extends to about 15°S [*Brandhorst*, 1971]. This water mass feeds shallow upwelling [*Brandhorst*, 1971] and is depicted by low surface salinity values, relative to offshore, salty subtropical surface waters [e.g., *Strub et al.*, 1998; *Torres et al.*, 2002]. Large-scale CO_2-undersaturated surface waters off northern Chile repeatedly coincide with the upwelling of this low-salinity water mass [*Lefèvre et al.*, 2002].

[11] Following the active phase of an upwelling event, the phytoplankton-poor, CO_2-supersaturated upwelled waters produce high levels of phytoplankton biomass (typically diatoms), and the biological uptake of nutrients (including CO_2) can eventually switch the direction of CO_2 fluxes [e.g., *Simpson and Zirino*, 1980]. However, low levels of dissolved iron may prevent the rapid interception of upwelled CO_2 by phytoplankton off central Chile (near 30°S [*Torres and Ampuero*, 2009]) and off Peru [*Friederich et al.*, 2008], and therefore carbon uptake by phytoplankton can be limited even before nitrate is depleted.

1.3. Patagonian Fjords of Southern Chile

[12] Large-scale wind circulation patterns do not promote coastal upwelling at latitudes higher than 40°S, in particular, in the Pacific region of Patagonia, which is characterized by intricate geography covering some 10^5 km^2 of coastal ocean. The Patagonian fjords and channels (42°S–56°S) are colder, less saline, and more stratified than the coastal areas affected by upwelling events. Certainly, at these cold and rainy latitudes, the enormous freshwater input into the coastal ocean because of high levels of precipitation [*Dávila et al.*, 2002] and meltwater from the Patagonian ice fields [*Rignot et al.*, 2003] has a dominant effect on hydrological processes and surface water properties. The elevated freshwater inputs enhance surface stratification and create strong haloclines in several fjords and estuaries of the region. By limiting the depth of turbulent mixing, stratification acts to confine primary producers to the near surface and isolates the surface layer from the CO_2-rich water below the pycnocline. By preventing mixing with deeper waters, these physical conditions support the biological sequestration of surface CO_2 and maintain a CO_2-depleted surface water layer (i.e., stratification separates production and respiration processes [see *Thomas et al.*, 2004]). Moreover, low-salinity waters are enriched with both silicic acid [*González et al.*, 2010; B. Reid, personal communication, 2010] and dissolved iron [*Gaiero et al.*, 2003], which may enhance diatom proliferation.

[13] The uptake or release of CO_2 by fjord surface waters largely depends on the dominant metabolic status of this top layer (i.e., autotrophy versus heterotrophy). CO_2 fluxes determined for the Atlantic side of the continental shelf of Patagonia (comprising 10^6 km^2) have shown that these areas are an important sink of CO_2 during warm periods [*Bianchi et al.*, 2005]. However, the overall contribution of the fjord

Table 1. Estimates of Surface Seawater pCO_2 Along the Coast of Chile Between 1995 and 2009[a]

Dates (dd/mm/yyyy)		Latitude	Surface Seawater pCO_2 Range	Atmospheric X_{CO2}			
From	To	(°S)	(μatm)	(ppm)	Parameter	Platform	Reference
23/02/1993	23/02/1993	53	321	354	C_T, A_T		Glodap database
15/05/1995	26/06/1995	43-28	376–551	358	C_T, A_T	R/V *Sonne*	*Takahashi et al.* [2009]
22/07/1996	27/07/1996	30–31	335–700	359	pH and A_T	R/V *Abate Molina*	*Torres* [2001]
11/01/1997	26/01/1997	24-22	237–637	361	pH and A_T	R/V *Abate Molina*	*Torres et al.* [2002]
27/01/1997	27/01/1997	24–28	279–418	361	pCO_2	R/V *Abate Molina*	*Lefèvre et al.* [2002]
28/01/1997	01/02/1997	30–31	249–922	361	pH and A_T	R/V *Abate Molina*	*Torres et al.* [2002]
01/07/1997	20/07/1997	24-22	369–605	361	pH and A_T	R/V *Abate Molina*	*Torres* [2001]
20/12/2001	22/12/2001	26–33	369–642	369	pCO_2	R/V *Abate Molina*	
28/06/2002	30/06/2002	47–53	236–430	370	pCO_2	R/V *Laurence M. Gould*	*Takahashi et al.*, [2009]
19/10/2003	24/10/2003	34–54	240–508	374	pCO_2 and C_T	R/V *Mirai*	
12/11/2004	12/11/2004	35	658	375	C_T, A_T	R/V *Atalante*	*Goyet et al*. [2009]
29/12/2004	05/01/2005	33–54	190–887	376	pCO_2	R/V *Ronald Brown*	
04/03/2005	07/03/2005	52–30	165–695	375	pCO_2	R/V *Hesperide*s	
11/01/2005	13/01/2005	54–55	244–323	375	pCO_2	R/V *Ronald Brown*	
13/03/2005	15/03/2005	55	234–311	376	pH and A_T	M/V *Chonos*	
04/07/2005	14/07/2005	50–54	166–415	377	pCO_2	R/V *Palme*r	*Takahashi et al.*, [2009]
07/07/2005	13/07/2005	42	286–605	377	pH and A_T	Huinay Marine Station	
26/07/2005	16/11/2005	21.35	278–978	378	pCO_2	Mooring	*Friederich et al.* [2008]
04/11/2005	14/11/2005	42	178–207	376	pH and A_T	Huinay Marine Station	
29/03/2006	05/04/2006	42	187–271	378	pH and A_T	Huinay Marine Station	
09/11/2006	12/11/2006	54	277–376	379	pH and A_T	M/V *Chonos*	*Frangopulos et al.* [2007]
11/09/2007	28/11/2007	30	362–931	381	pH and A_T	Stella Maris II	*Torres and Ampuero* [2009]
14/02/2008	01/03/2008	55-28	110–766	382	pCO_2	R/V *Ronald Brown*	*Takahashi et al.* [2009]
05/03/2009	15/03/2009	55-24	170–424	384	pCO_2 and A_T	R/V *Hesperides*	

[a]Plotted in Figure 1. Atmospheric CO_2 molar fractions correspond to a southern Patagonia monitoring base (54.9°S and 68.5°W [*Globalview-CO2*, 2009]).

system of Pacific Patagonia as a source or sink of CO_2 has not been determined.

2. Methods

2.1. ΔpCO_2 Data Synthesis

[14] CO_2 data used in this study were obtained from various expeditions carried out along the Chilean coast between 1996 and 2009 (Table 1). Most of the data correspond to pCO_2 measurements obtained by means of air-sea equilibration methods coupled with a nondispersive infrared CO_2 gas analyzer [e.g., *Dickson and Goyet*, 1994]. Additional estimates of pCO_2 from pH@25°C and total alkalinity (A_T) were determined using the CO2SYS program [*Lewis and Wallace*, 1998] with Mehrbach solubility constants [*Mehrbach et al.*, 1973] refitted by *Dickson and Millero* [1987]. In order to estimate ΔpCO_2, records of the atmospheric pCO_2 level were subtracted from the surface seawater pCO_2 (Table 1). When atmospheric pCO_2 data were not measured (see Table 1), atmospheric CO_2 molar fraction (X_{CO2}) data from Patagonia (54.87°S and 68.48°W) were obtained from the Globalview-CO_2 database [*Globalview-Co*$_2$, 2009].

2.2. Estimation of CO_2 Flux at the Air-sea Interface

[15] The flux of CO_2 (FCO_2) across the air-sea interface was determined for those expeditions in which ΔpCO_2, wind speed, temperature, and salinity data were available (n = 4; Table 1), using the bulk formula: $FCO_2 = k \times s \times \Delta pCO_2$, where k is the gas transfer velocity (i.e., Wanninkhof's quadratic relationship for short-term, shipboard wind speed [*Wanninkhof*, 1992]), s is the CO_2 solubility and ΔpCO_2 is the difference in the CO_2 partial pressure between surface water and air. In order to compare data collected from different cruise tracks and at different spatial resolution, data were averaged every 1° latitude.

2.3. Salinity-Alkalinity Relationship and Calculation of C_T and ΔC_T

[16] The salinity-alkalinity relationship was used to calculate total carbon (C_T, or DIC) from paired pCO_2 and salinity data, using the CO2SYS program [*Lewis and Wallace*, 1998] with the Mehrbach solubility constant [*Mehrbach et al.*, 1973] refitted by *Dickson and Millero* [1987]. Surface water samples collected for A_T measurements during the Humboldt 2009 expedition (R/V *Hesperides*; March 2009) were analyzed following *Haraldsson et al.* [1997]. The measured surface A_T was strongly associated with salinity (R^2 = 0.99) in fjord waters. The regression obtained (A_T (μeq. kg^{-1}) = 61.9 × Salinity + 151), was very similar to that derived from the pCO_2 and C_T paired data measured during the Beagle Expedition (R/V *Mirai*) from 36°S to 54°S (A_T (μeq. kg^{-1}) = 61.8 × salinity + 145). Therefore, we used the former relationship to estimate A_T from salinity, and to estimate the rest of the carbonate system parameters for the historic data (i.e., from salinity and pCO_2 paired data).

[17] The difference between C_T calculated from corresponding surface water pCO_2 and atmospheric pCO_2 (using A_T derived from the A_T-salinity relationship) is designated ΔC_T. The ΔC_T is interpreted as a proxy for the apparent dissolved inorganic carbon production, revealing the degree of enrichment (positive C_T) or depletion (negative C_T).

2.4. Effect of Phytoplankton on pCO_2 in Estuarine and Marine Waters

[18] We assessed the effect of carbon fixation by phytoplankton on pCO_2 by running a numerical model (CO2SYS program) in which C_T was either removed or added from two water bodies with different salinity, defined here as 25 and 35. Initial conditions assumed full saturation with atmospheric

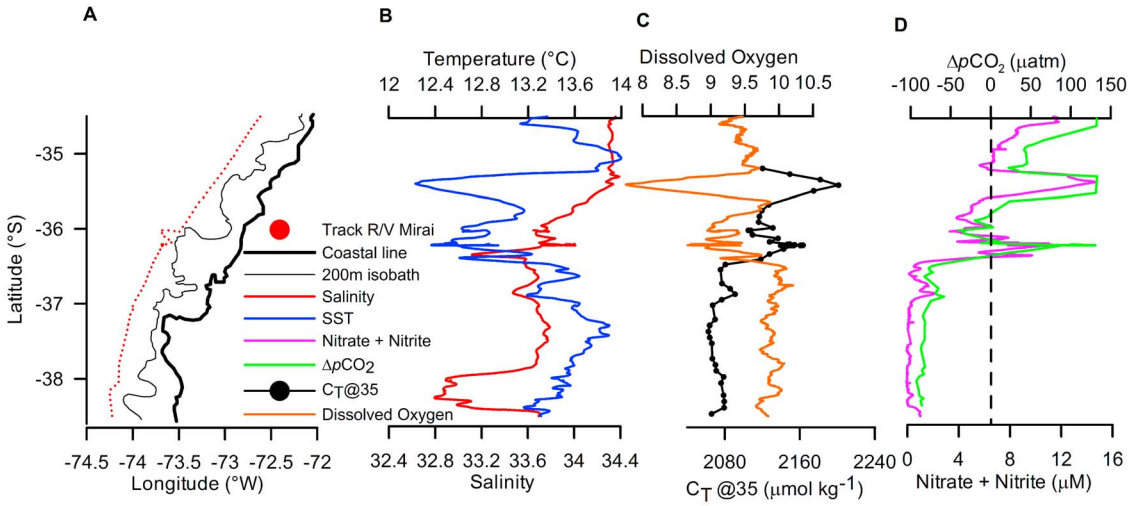

Figure 2. Underway surface water measurements off central Chile during October 2003 (Beagle Expedition, R/V *Mirai*). (a) Research vessels tracks, 200 isobath and coast line. (b) SST and SSS. (c) Dissolved oxygen and C_T normalized to salinity 35 (C_T@35). (d) ΔpCO_2 and nitrate plus nitrite.

CO_2 ($\Delta pCO_2 = 0$ and $\Delta C_T = 0$), but with different salinity (and alkalinity proportional to salinity; see section 2.3). The model assumed an initial nitrate level of 10 μmol kg^{-1} and pCO_2 of 380 μatm. Temperature and pressure were assumed constant (12°C and 1 m depth). The calculations were determined using CO2SYS [*Lewis and Wallace*, 1998] with the Mehrbach solubility constants [*Mehrbach et al.*, 1973] refitted by *Dickson and Millero* [1987], and assuming that (1) the A_T variability is exclusively caused by increases or decreases in nitrate; (2) the changes in nitrate (ΔNO_3^-) and carbon (ΔC_T) are exclusively caused by photosynthesis and respiration in Redfield proportions.

2.5. Estimation of Primary Production and Community Respiration in a Stratified Fjord (Puyuhuapi Fjord) During the Austral Summer Period

[19] Gross primary production (GPP) and community respiration (CR) were estimated from changes in dissolved oxygen (DO) concentrations observed in situ light and dark incubations [*Strickland*, 1960]. Water sampled via Niskin bottles was transferred to 125 mL nominal borosilicate bottles (gravimetrically calibrated). Water samples were collected at dawn and were incubated during the entire light period. All incubations were performed with five replicates. The light and dark bottles were incubated using a surface-tethered mooring system. Dissolved oxygen was measured by a manual method based on the Winkler procedure, using a piston burette.

3. Results

3.1. Surface ΔpCO_2 Along the Coast Off Chile

[20] Surface pCO_2 from expeditions along the Chilean coast showed the predominance of CO_2-supersaturated surface waters from 21°S to 37°S (Figure 1). Very high CO_2 supersaturation ($\Delta pCO_2 > 400$ μatm) was observed at the two major upwelling centers off Concepción and Coquimbo during the austral spring-summer period (Figure 1). South of ~37°S, pCO_2 decreased sharply during the austral spring-summer period. A close inspection of this area (Figure 2a) showed that north of 37°S, the cold and salty (>34.2) surface waters (Figure 2b) were enriched in dissolved inorganic carbon (C_T) and poorly oxygenated (Figure 2c). This water was also highly enriched in nitrate and strongly CO_2 supersaturated (Figure 2d). Conversely, surface waters at latitudes >37°S were less salty and more oxygenated, with lower levels of C_T, strongly undersaturated in CO_2, and depleted in nitrate (Figure 2). Several expeditions at the Coquimbo upwelling center (Figures 1 and 3) suggested that maximum levels of surface water pCO_2 occurred in relatively cold water near the

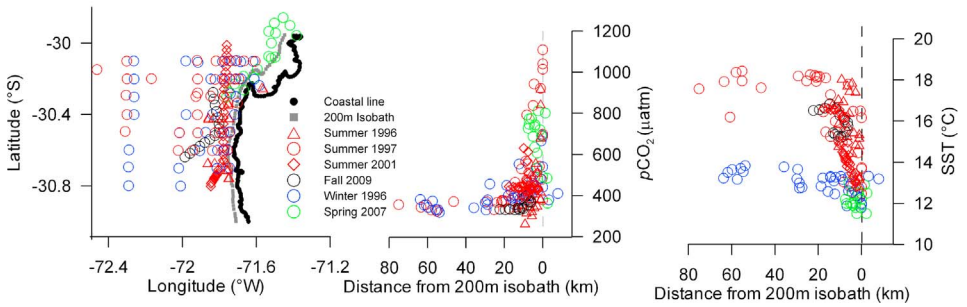

Figure 3. Surface water pCO_2 and SST from various expeditions off 30°S (Coquimbo Upwelling System).

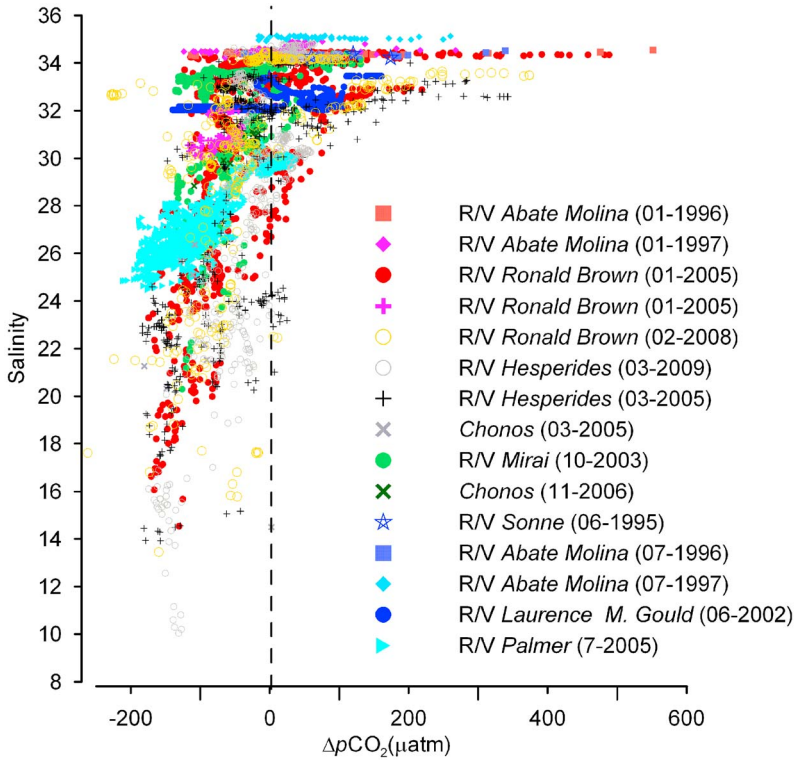

Figure 4. Relationship between salinity and ΔpCO_2 in surface coastal waters of Chile. Note that low-salinity water (salinity < 28) is normally undersaturated in CO_2.

edge of the continental shelf (Figure 3) during the spring-summer; coastal water inside the bays exhibited lower pCO_2 however (Figure 3).

[21] The Patagonian fjord region (42°S–55°S) showed a prevalence of CO_2 undersaturation, particularly at latitudes higher than 47°S (Figure 1). The shallow waters of the inner Chiloe archipelago (from 42.2 to 43.0°S, where mean bottom depth is ~95m, with a significant portion of very shallow areas <20 m depth) and waters north of the windy Golfo de Penas 46°S were supersaturated in CO_2 (ΔpCO_2 between 50 and 200 μatm; Figure 1). Conversely, surface waters were persistently CO_2-undersaturated near the Southern Ice field (e.g., 48°S–52°S; Figure 1), where the coastal ocean receives high inputs of freshwater from glaciers. In general, low-salinity surface water in the fjords and channels of Patagonia (e.g., salinity <28) are strongly undersaturated in CO_2 (Figure 4).

[22] An offshore transect at 53°S (Figure 5a) showed that subantarctic surface water (SSW) was relatively low in pCO_2 (slightly CO_2 undersaturated) during the austral summer, particularly in the low-salinity surface waters found closer to the continent shelf edge (Figure 5b). The maximum nitrate, phosphate, and C_T levels were located along the offshore side of the transect, associated with less CO_2-undersaturated surface waters (Figures 5b and 5c). Despite of the high levels of nitrate and phosphate, the surface-dissolved silicate (DSi) was invariably low (<2 μM, Figure 5c).

3.2. Seasonal Variability of ΔpCO_2 Within Fjords and Channels of Patagonia

[23] Repeated surface (5 m) ΔpCO_2 estimates in a northern Patagonia fjord (Huinay Marine Station at 42°S, Figure 1) during the austral winter (July), spring (November), and late summer (March) showed that surface waters were undersaturated in CO_2 during spring and summer, but they were CO_2 supersaturated in winter. A repeated transect of underway pCO_2 measurements near the Southern Patagonia Ice Fields (SPIF; Figure 6) suggested a similar pattern: while particularly low surface water pCO_2 values occurred in spring and summer (i.e., larger CO_2 undersaturation), maximum surface pCO_2 (close to atmospheric pCO_2 level) occurs during winter (Figure 6b). The reduction of surface seawater salinity (SSS) from spring to summer was associated with an increment in SST (Figures 6c and 6d). However, individual peaks of low SSS were often associated with relatively cold waters, a phenomenon probably caused by the input of recently melted glacial ice. At ~50°S, at the mouth of two fjords connected to the Southern Ice Field, winter SSS values were higher than in spring and summer (Figure 6c and Table 2); this seasonal variability is most probably caused by a high input of freshwater during the warm periods. It is worth noting that the extreme surface water CO_2 undersaturation, which occurred near 50°S during February 2008, was associated with low salinity but particularly cold water at 50°S (Figures 6b–6d). In general, peaks of maximum CO_2 undersaturation occurred in low-salinity surface waters (Figures 6b and 6c).

[24] During the Beagle 2003 (R/V *Mirai*) and Humboldt 2009 (R/V *Hesperides*) expeditions, A_T showed a linear relationship with SSS (section 2.3 and Figure 6e). At 10°C, the winter pCO_2 was maximum (Figure 6f), and the apparent consumption of CO_2 was minimum (ΔC_T closer to zero; Figure 6g). Along the northern side of the "Angostura Inglesa" strait, pCO_2 at 10°C was substantially lower during austral summer (December–March) than in spring (October),

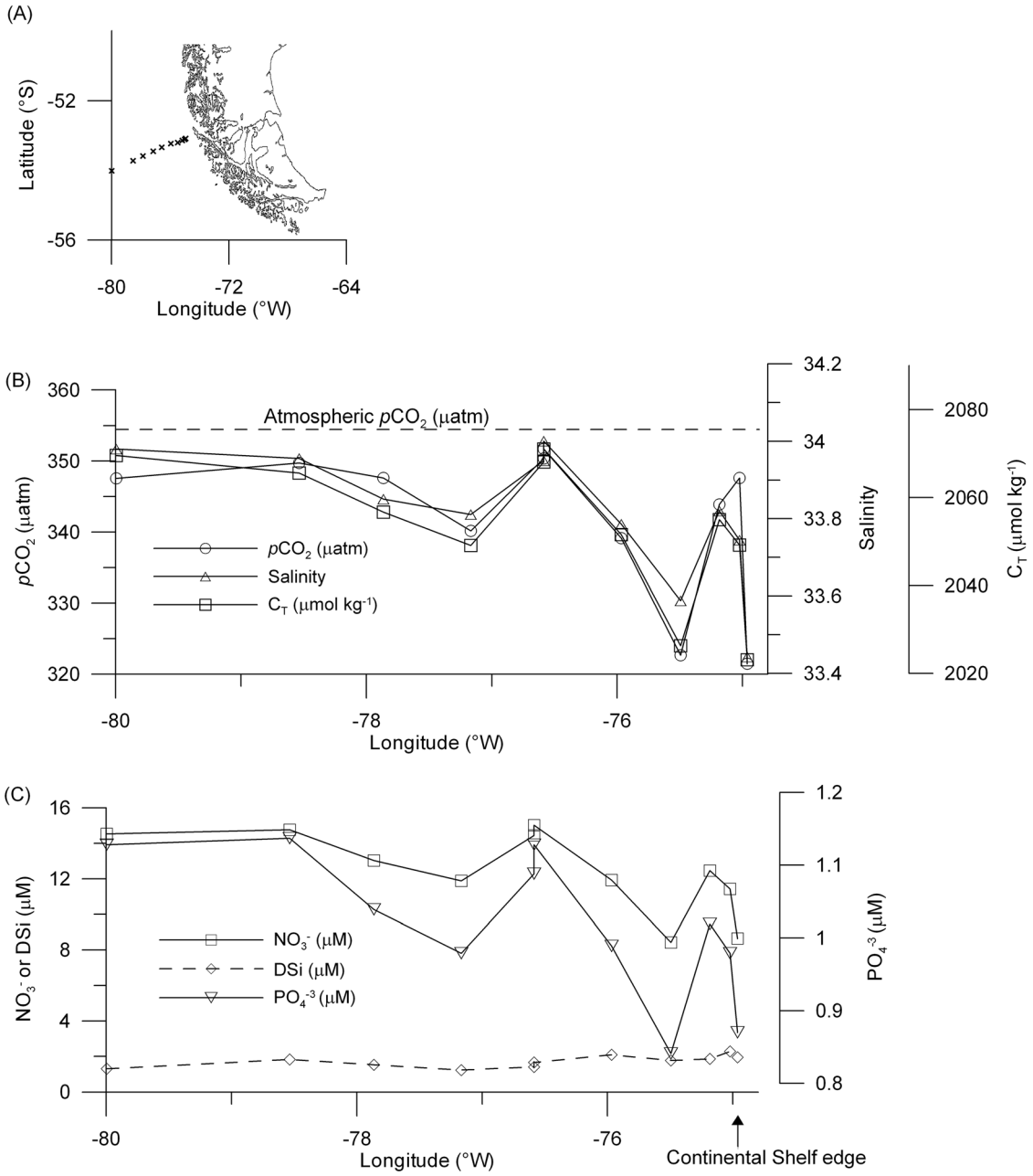

Figure 5. Across shore transect (53°S) of surface water (subantarctic surface water, SSW) from the edge of the continental shelf of Patagonia to 80°W during the austral summer 1993 (Global Ocean Data Analysis Project database). (a) Stations location. (b) Across-shore distributions of pCO_2, C_T, and salinity. (c) Across-shore distribution of nitrate (NO_3^-), phosphate (PO_4^{3-}), and dissolved silicate ($Si(OH)_4$).

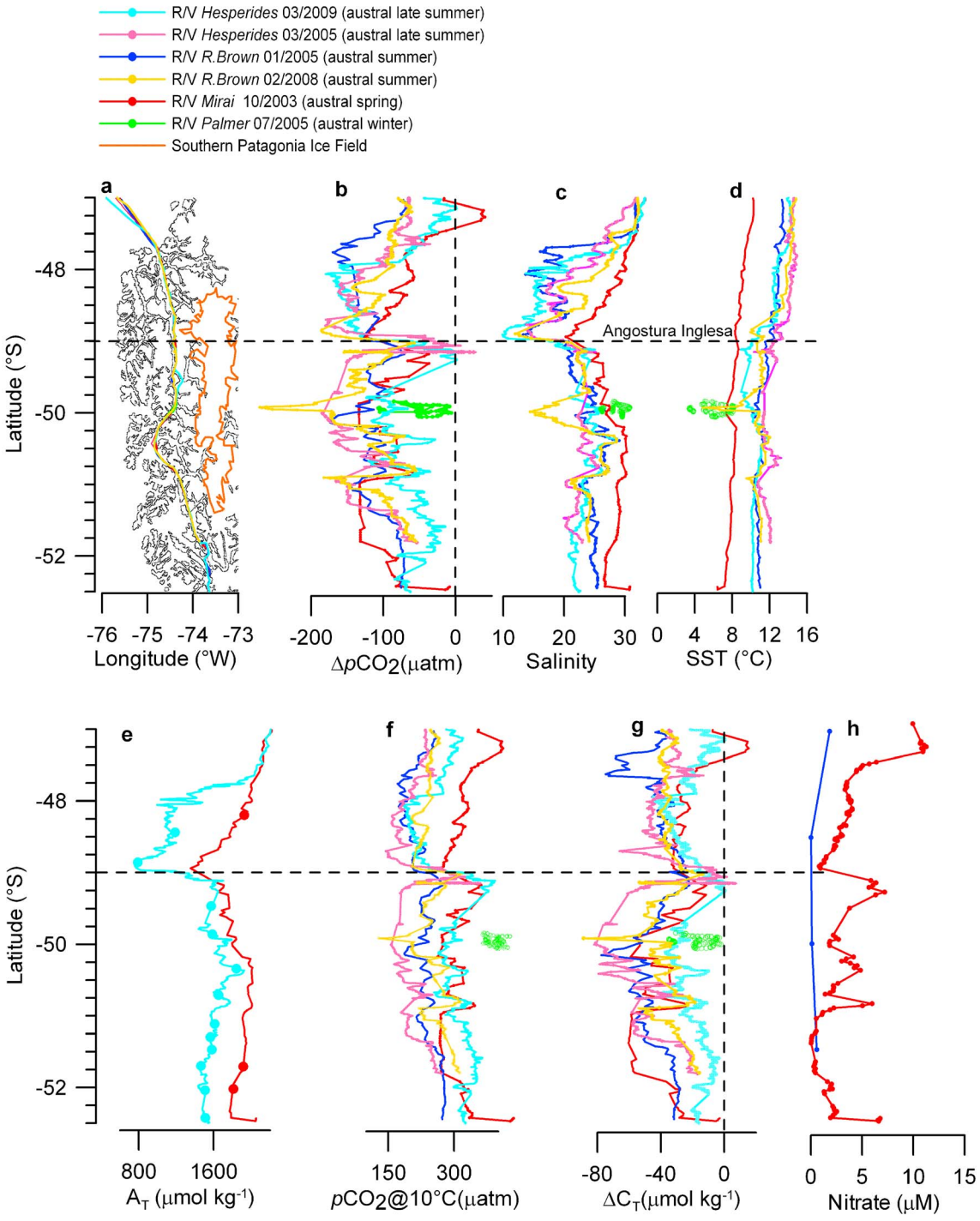

Figure 6. Underway surface water measurements within Patagonian channels during various expeditions. The horizontal dashed line depicts the location of a major topographic constriction (Angostura Inglesa). (a) The coast line (black line), the Southern Ice Field (orange line), and the ~700 km long transect (a particular color identifies each expedition). (b-h) Measurements of underway ΔpCO_2, sea surface salinity (SSS), sea surface temperature (SST), total alkalinity (A_T), and pCO_2 at 10°C (pCO_2@10°C) and ΔC_T (as defined in section 2.3) and nitrate concentration, respectively. In Figure 6e, dots depict estimations of A_T and the lines depict A_T values calculated from A_T-salinity relationship (see section 2.3).

Table 2. Observations of Seawater Surface Temperature (SST), Seawater Surface Salinity (SSS), and ΔpCO_2 at 50.0°S and 74.4°W During the Austral Winter, Austral Spring, and Austral Summer

Cruise	SST	SSS	ΔpCO_2
R/V *Palmer* (6–2005)	6.0 ± 1.6	28.6 ± 1.4	−52 ± 32
R/V *Mirai* (10–2003)	7.4 ± 0.1	27.0 ± 0.5	−134 ± 0
R/V *Ronald Brown* (1–2005)	11.0 ± 0.6	23.5 ± 1.7	−123 ± 18
R/V *Hesperides* (3–2005)	11.4 ± 0.1	22.4 ± 0.3	−182 ± 1
R/V *Hesperides* (3–2009)	10.1 ± 0.4	24.7 ± 1.0	−90 ± 9

Table 3. Statistics and Correlation Matrix of Hydrographic and Surface Water pCO_2 Data of Two Glacial Fiords (Penguin and Europa, 50°S) During Austral Winter (R/V *Palmer*, 2005)[a]

	Min	Max	Range	SST (R)	SSS (R)
SST (°C)	−1.2	8.2	9.4	1	
SSS	24.5	30.8	6.3	0.5	1
pCO_2@SST (μatm)	166	371	205	0.7	0.8
pCO_2@10°C (μatm)	202	419	202	0.1	0.6

[a]Correlations (R) are statistically significant ($p < 0.05$), estimated from a matrix of 1763 observations.

while ΔC_T during the austral summer was not always higher (in absolute value) than during the spring period. This suggests a similar consumption of CO_2 during both periods (austral spring and summer) even though surface nitrate was often higher during austral spring (R/V *Mirai* data) compared with the austral summer (R/V *Ronald Brown* data; Figure 6h).

3.3. Spatial Variability of ΔpCO_2 Within Patagonian Fjords

[25] pCO_2 variability off the SPIF area (Figure 6) was similar between surveys (note the similarity in the spatial variability of pCO_2 at 10°C in spring and summer surveys between 49°S and 51°S, Figure 6f). Glacial fjords were associated with intense spatial gradients in surface water pCO_2. Surface waters at the head of the fjord were characterized by an intense undersaturation in CO_2, contrasting with higher surface water pCO_2 values at the fiord's mouth (Figure 7a). During austral winter in the Penguin and Europa glacial fjords, the cold and less salty inner fjord waters exhibited lower surface water pCO_2 than the warmer and saltier surface waters at the fjord's mouth (Figure 7b). Indeed, surface water pCO_2 was positively correlated with both temperature and salinity (Table 3). Because the SST range along the fjords exceeds 9°C (Table 3), low pCO_2 in cold, low-salinity waters could be an effect of temperature. However, the correlation between salinity and pCO_2 persists even when pCO_2 is corrected for temperature (pCO_2 at 10°C; Table 3). Vertical pCO_2 profiles along a glacial fjord within the Magellan strait (54°S, during austral spring 2005; Figure 8) also showed along fjord CO_2 gradients, from minimum pCO_2 and apparent oxygen utilization (AOU) values at the head of the fjord to higher levels at the fjord's mouth. During this campaign, we observed a close connection between surface water O_2 supersaturation (negative AOU levels) and CO_2 undersaturation, indicating strong autotrophic behavior in the surface layer (Figure 8). Accordingly, the estimation of phytoplankton productivity and community respiration of surface water (5 m) in the Seno Ballena fjord during the austral spring (2005) showed a GPP/CR ratio between 4 and 16 (n = 3, data not shown).

[26] A high-resolution vertical profile taken at the Puyuhuapi fiord (44°S) during the austral summer of 2007 showed that the warm halocline that characterized the upper 9 m depth layer (Figures 9a and 9b) had invariably high pH values (Figure 9c) and was strongly undersaturated in CO_2 (Figure 9d). Meanwhile, daily in situ primary productivity experiments showed high rates of phytoplankton production (Figure 9e) compared with community respiration (Figure 9f) within the low pCO_2 surface layer (i.e., top 9 m). Thus, biological consumption of C_T (GPP/CR > 1, Figure 9g) probably maintained the low pCO_2 in surface waters. The ΔC_T (section 2.3, Figure 9h) and dissolved oxygen (Figure 8i) reveal autotrophic behavior in the low-salinity layer. Based on the net productivity (i.e., GPP-CR) of these low-salinity surface waters of approximately 3–5 mg C L^{-1} h^{-1}, we estimate that phytoplankton productivity could deplete C_T by about 50 μmol kg^{-1} (ΔC_T = −50) over approximately 5–8 days. In general, minimum values of

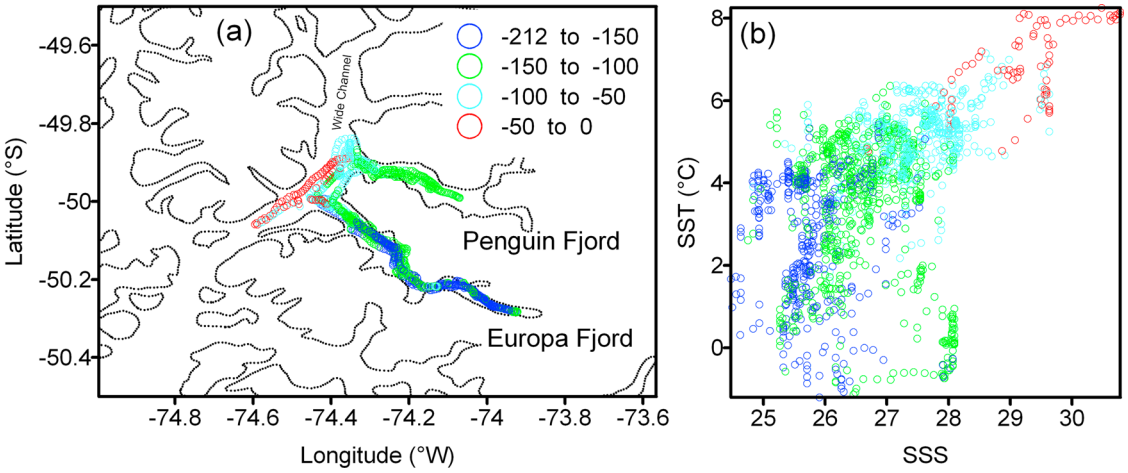

Figure 7. (a) ΔpCO_2 along the Penguin and Europa fjords (~50°S) and (b) the relationship between SSS, SST, and pCO_2 in both fjords.

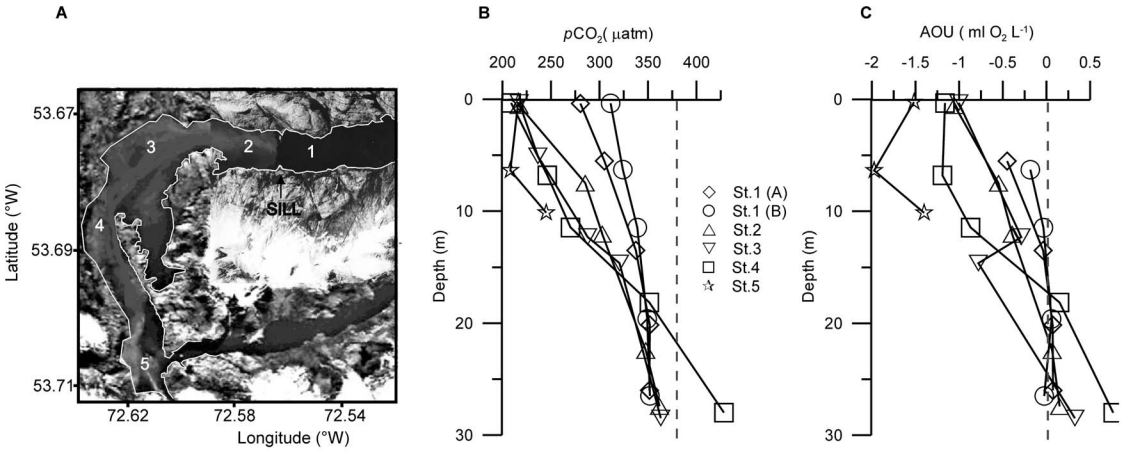

Figure 8. (a) A map of the Ballena Fjord and the sampling stations. Vertical distributions of (b) pCO_2 and (c) AOU along the Ballena Fjord (~54°S) during November 2005 (austral spring). Vertical profiles at each station are shown; the dashed line shows saturation levels for O_2 and CO_2.

pCO_2 occurred in highly productive, low-salinity surface waters segregated by a strong halocline from the deeper heterotrophic layer (denser, saltier, and CO_2-supersaturated; Figure 9).

3.4. Theoretical Effect of Phytoplankton Carbon Fixation on pCO_2 in Estuarine and Marine Water

[27] The modeling results suggested that the pCO_2 decline associated with uptake of macronutrients (e.g., C_T, nitrate) by primary producers was more intense in estuarine waters than in more salty waters (Figure 10a). Similarly, the remineralization of organic matter resulted in a greater increase in ΔC_T in estuarine water compared with marine waters (Figure 10a). Note that the relationship between pCO_2 and ΔC_T is asymmetric (Figure 10a); the release of C_T increased pCO_2 to a higher degree than the reduction of pCO_2 resulting from C_T consumption. This asymmetry was due to the increase in the Revelle Factor with increasing pCO_2 [*Broecker et al.*, 1979], thus reducing the buffer capacity of seawater (Figure 10b). This last phenomenon was particularly evident in low-salinity waters; note that the slope in the Revelle Factor-ΔC_T relationship was higher for estuarine (m = 0.06) than for marine waters (m = 0.03; see Figure 9b).

3.5. CO_2 Exchanges at the Air-Sea Interface Along the Chilean Coast

[28] Coastal ΔpCO_2 determined during four surveys in the spring-summer period (Figure 11) showed large deviations

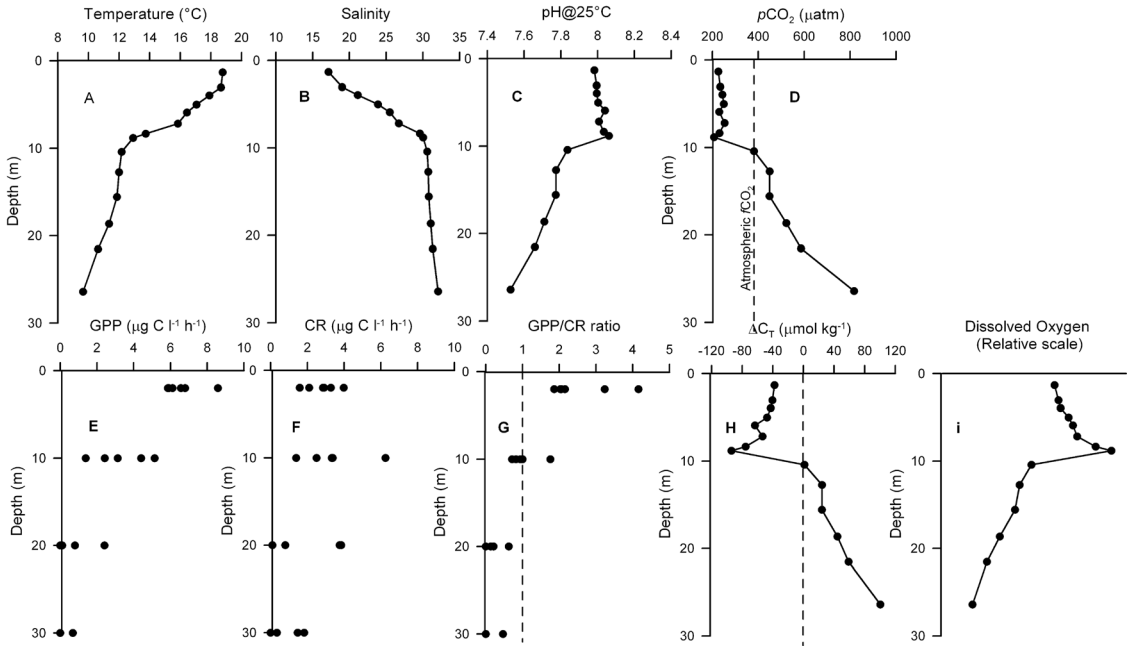

Figure 9. High-resolution profile of the Puyuhuapi Fjord (~44°S). (a) SST, (b) Salinity, (c) pH at 25°C, (d) pCO_2, (e) gross primary productivity, (f) community respiration, (g) GPP/CR ratio, (h) ΔC_T, and (i) dissolved oxygen.

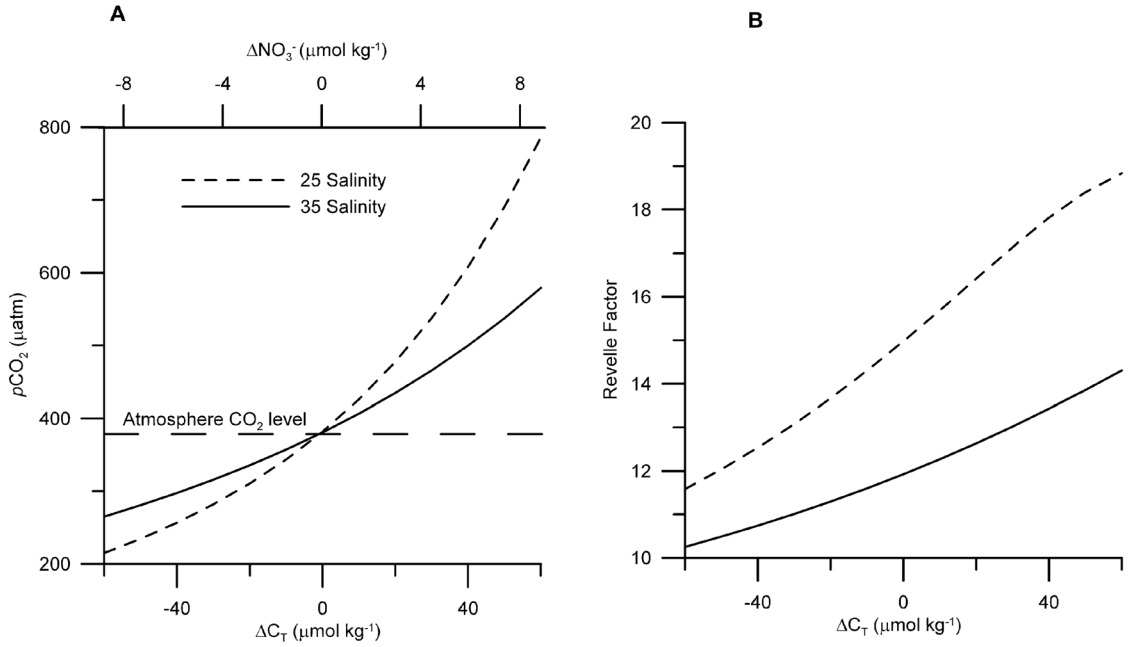

Figure 10. Effects of the gains or losses of C_T on (a) pCO_2 and (b) Revelle Factor in both marine (salinity 35) and estuarine waters (salinity 25); see section 2.4. Note that $\Delta C_T = 0$ depicts the initial conditions when both waters are fully CO_2 equilibrated with the atmosphere (i.e., pCO_2 of water was equal to the atmospheric pCO_2). Note that top x axis shows the changes in nitrate (ΔNO_3^-) associated with the changes in C_T (ΔC_T; lower x axis) following Redfield proportions (C:N = 106:16). Linear regressions fitted for the Revelle Factor (RF)-ΔC_T relationships are represented by $RF = 0.03 \times \Delta C_T + 12$ and $RF = 0.06 \times \Delta C_T + 15$, for marine (35 salinity) and estuarine (25 salinity) waters, respectively.

from saturation levels (Figure 11b). The SST decreased toward high latitudes (Figure 11c). Wind speed measured in eight coastal meteorological stations in Patagonia suggest that wind speeds within fjords and channels were highly variable (black square symbol, Figure 11d; see Table 4). The mean wind speed was approximately 5 m s^{-1}, with minimum values at topographically wind-protected areas (e.g., such as in the innerfjord of Seno Eyre and Puerto Eden; Table 4) and maximum values were from areas well exposed to oceanic winds, at the southernmost station (i.e., Faro Diego Ramirez, Table 4) and at Golfo de Penas (Faro Raper, Table 4). Onboard wind speed records showed a large range of variability, but maximum wind speed values up to 26 m s^{-1} were recorded only at higher latitudes (Figure 11d).

[29] Latitudinal SST gradients (Figure 11c) and the maximum wind speed event in southern Patagonia (Figure 11d) yielded a north to south gradient in the CO_2 solubility coefficients (α; Figure 11e) and the gas exchange coefficients derived from onboard records (k; Figure 11f). This latitudinal gradient in α, k, and CO_2 undersaturation yields a large CO_2 flux ($\alpha \times k \times \Delta pCO_2$) toward the coastal ocean of Patagonia (Figure 11e).

[30] The mean ± SD CO_2 flux in Patagonia (from 42°S to 55°S) based on 1° latitude binned averages for the four available surveys (Figure 11a) was −15 ± 17 mmol m^{-2} d^{-1}. This mean flux was associated with a high mean ± SD CO_2 undersaturation (−51 ± 62 μatm) in surface waters, a high mean CO_2 solubility (0.044 ± 0.003 mol l^{-1} atm^{-1}), and a particularly high mean K (27 ± 13 cm h^{-1}) at these cold, windy latitudes. The estimation of mean CO_2 fluxes across the upwelling areas of central and northern Chile were precluded by the paucity of data [see *Torres et al.*, 1999].

4. Discussion

4.1. Strong Coastal Surface Water CO_2 Supersaturation and Deep Upwelling Off Chile

[31] Particularly high ΔpCO_2 values in surface waters off Concepción (37°S–35°S) during austral spring-summer (Figures 1 and 2) were associated with the upwelling of salty (e.g., >34.2), cold, and poorly oxygenated water (Figure 2). This suggests that the upwelled water was enriched in ESSW [*Brandhorst*, 1971]. The ESSW is advected south in the Chile-Peru undercurrent [*Silva and Neshyba*, 1979] and feeds the deep upwelling of the entire Chilean upwelling region [see *Brandhorst*, 1971; *Strub et al.*, 1998]. Because the highest pCO_2 of the South Pacific eastern boundary current occurs at the core of the cold and salty ESSW [e.g., *Torres et al.*, 2002], deep upwelling (i.e., from the undercurrent) may explain the very high ΔpCO_2 surface values (e.g., Concepción, Coquimbo, and Antofagasta in Figure 1; see review by *Strub et al.* [1998]). At 37°S, the upwelling of water from the undercurrent toward the shelf is expected to be enhanced by a deep-water cyclonic eddy [*Leth and Middleton*, 2004]. This particularly deep upwelling may explain the strong CO_2 outgassing from coastal waters at 37°S, and this upwelled water is expected to be advected north through the meandering Chile coastal current [*Leth and Middleton*, 2004].

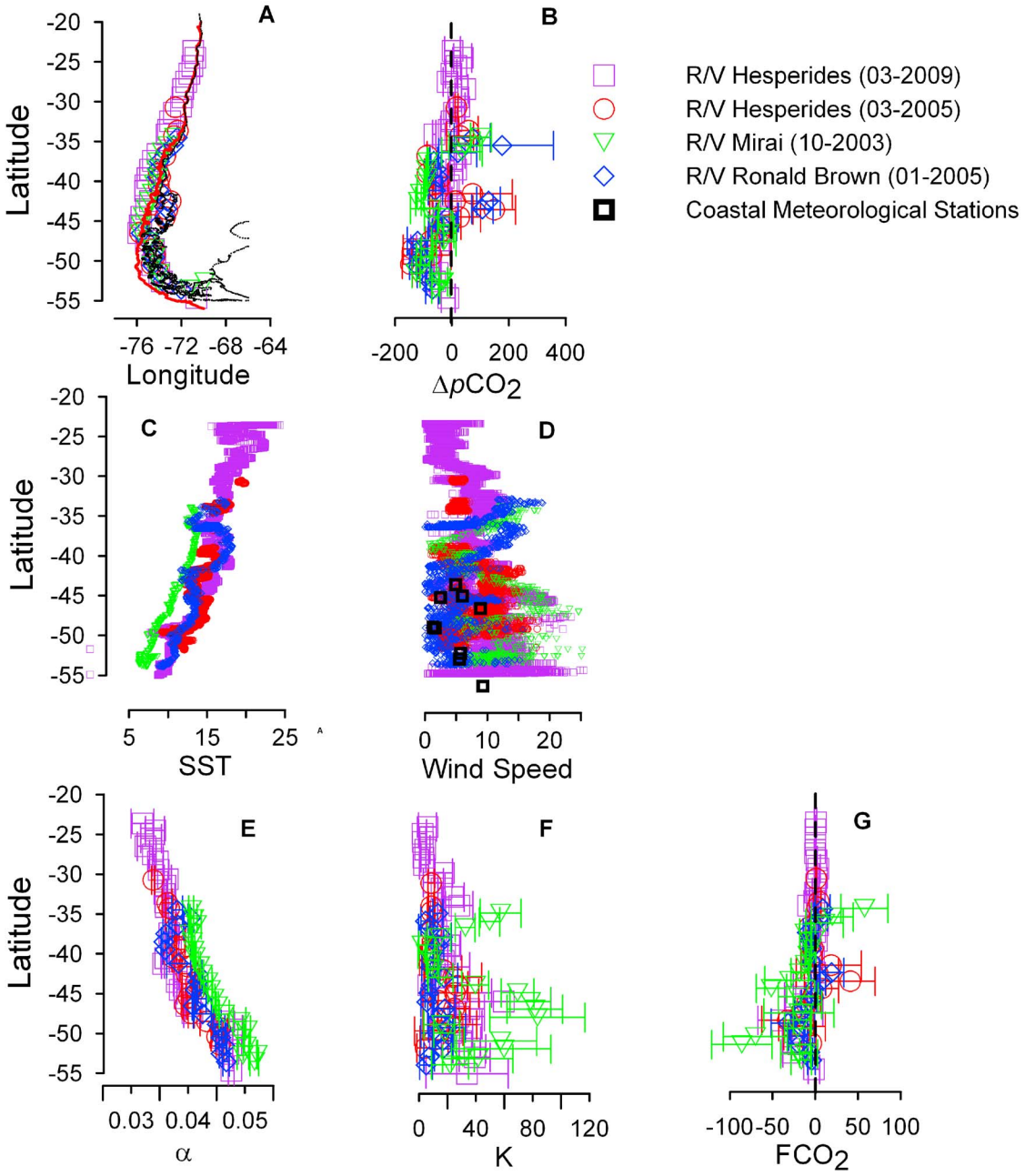

Figure 11. CO_2 fluxes off Chile: (a) map, (b) 1° average ΔpCO_2, (c) raw SST, (d) raw wind speed, (e) 1° average CO_2 solubility, (f) 1° average k solubility, and (g) 1° average CO_2 flux (negative values depict sink).

[32] During spring-summer, a strong tendency toward thermal stratification coincided with the period of intense wind-forced upwelling, thus higher pCO_2 levels are associated with the erosion of the thermocline/pycnocline (i.e., reduction in water column stratification) close to the edge of the continental shelf (Figure 3). This maximum coastal surface water pCO_2 set up strong across-shore pCO_2 gradients during active upwelling [e.g., *Torres et al.*, 1999, 2002], as has been reported for other coastal upwelling systems (e.g., off Point St. George, California [*Feely et al.*, 2008]).

[33] High levels of CO_2 undersaturation may also occur within the main upwelling centers (e.g., Concepción, Coquimbo, and Antofagasta, Figure 1), probably as a consequence of photosynthesis in stratified coastal waters (e.g., at fronts, within bays, during relaxation of the upwelling [see *Lefèvre et al.*, 2002; *Torres et al.*, 1999, 2002; *Torres and Ampuero*, 2009]). However, CO_2 undersaturation levels were less intense than those observed in the southern portion of the study area (e.g., between 47°S and 51°S; Figure 1). This pattern could be caused by the interaction of several factors, including the more intense stratification and the more efficient reduction of pCO_2 per utilization of C_T (and other nutrients) by photosynthesis in the low-salinity waters of southern Chile (see section 3.4 and Figure 10).

Table 4. Wind Speed Measured at Meteorological Stations in Patagonian Fjords and Channels

Meteorological Station	Latitude (°S)	Longitude (°W)	Period	Wind Speed ($m\ s^{-1}$)	Data Source
Raul Marin Balmaceda	43.8	73.1	2001–2005	4.9 ± 4.5 (n = 55,154)	Trapananda, UACh
Islote Rosas (Canal Moraleda)	45.2	73.6	Sep 1998 to Feb 1999	6.0 ± 4.4 (n = 3662)	SHOA
Isla Mitahue	45.4	73.8	Jul 2002 to Nov 2002	2.5 ± 1.5 (n = 1852)	SHOA
Faro Cabo Raper (Golfo de Penas)	46.8	75.6	2003–2005	8.9 ± 5.4 (n = 5031)	Servicio Meteorológico de la Armada
Puerto Eden	49.1	74.4	Jul 2005 to Dec 2005	1.3 ± 1.4 (n = 642)	Servicio Meteorológico de la Armada
Seno Eyre	49.3	74.1	Oct 1996	1.7 ± 0.7 (n = 118)	SHOA
Punta Delgada (Magellan Strait)	52.5	69.5	Oct 1997 to Dec 1997	5.7 ± 3.2 (n = 3186)	SHOA
St. Jorge C. Schythe (Magellan Strait)	53.1	70.9	2001–2005	5.5	*Butorovic* [2003, 2005]
Faro Diego Ramirez	56.5	68.7	2003–2005	9.3 ± 5.3 (n = 1852)	Servicio Meteorológico de la Armada

[34] At latitudes higher than 37°S, surface water was predominantly undersaturated in CO_2 during spring-summer. Upwelling events still occur between 38°S and 40°S [*Figueroa and Moffat*; 2000], but the upwelling centers seems to be located over the continental shelf [*Atkinson et al.*, 2002]. Within these centers, oxygen-poor ESSW intrudes into the coastal waters, sometimes affecting surface waters [*Atkinson et al.*, 2002] and potentially leading to a strong CO_2 outgassing. However, we cannot assess this last hypothesis because the cruise tracks (Figure 1) did not enter the continental shelf in this area (38°S–40°S). In general, the coastal water dynamics of the southern portion of the upwelling region of Chile (38°S–40°S) is highly complex because of the influences of the coastal upwelling, the presence of offshore eddies, the influx of runoff at these rainy latitudes, and the broad continental shelf. This complexity seems to be associated with high biological production [*Atkinson et al.*, 2002], which could explain the persistence of waters highly undersaturated in CO_2 in this area (Figure 1).

[35] *Chaigneau and Pizarro* [2005] have shown that oceanic SSW transported within the Antarctic Circumpolar Current can be trapped within the Chile-Peru Current or Cape Horn Current at approximately 44°S, and advected along the coast to lower and higher latitudes, respectively. Consequently, surface water flowing north along the coast (e.g., from 44°S to 38°S) may correspond to the early encounter of oceanic SSW with the coastal environment. This coastal environment is characterized by influx of both (1) continental nutrients (e.g., dissolved iron and dissolved silica derived from a broad continental shelf and river discharges at these rainy latitudes) and (2) middepth ocean nutrients derived from the upwelling of relatively salty and poorly oxygenated ESSW. The recurrent strong CO_2 undersaturation (Figure 1) and postbloom characteristics, such as nutrient depletion (Figure 2), between 44°S and 38°S could be caused by a particularly high productivity triggered by the mixing of oceanic (i.e., nitrate-rich and slightly CO_2 undersaturated SSW, Figure 5) and iron-enriched coastal waters. Support for this hypothesis includes the following:

[36] 1. Preserved diatom assemblages in surface sediments off Chile [*Romero and Hebbeln*, 2003] shows an abrupt decrease of *Chaetoceros* spores south of 38°S off Chile, coupled with the enhanced contribution of *Thalassiosira* spp. This latter diatom is characteristic of high-productivity, low-temperature waters, suggesting a contribution from the iron-limited, nutrient-rich Antarctic Circumpolar Water [*Romero and Hebbeln*, 2003].

[37] 2. The net flux of CO_2 from the atmosphere to the ocean close to southern Pacific Patagonia (approximately below 42°S) is particularly intense compared with offshore observations (e.g., between 80°W and 110°W [*Takahashi et al.*, 2009]). This suggests that the capacity of the southeastern Pacific Ocean to sequester CO_2 intensifies as oceanic water moves closer to the continent. Accordingly, the across-shore transect off Patagonia (Figure 5) showed that surface seawater pCO_2 tends to decrease toward the continental shelf.

4.2. Patagonian Fjords

4.2.1. Contrasting pCO_2 Levels Between Oceanic SSW and Coastal Waters of Patagonia: The Freshwater Factor

[38] The high seasonal variability of solar irradiance in Patagonia is expected to force a concomitant variation in surface water productivity and in surface water nutrients concentrations (e.g., nutrient depletion during summer, after the spring bloom). Conversely, open ocean surface waters off Patagonia (Figure 5) were nutrient-rich during the height of the austral summer (Figure 5c), with very low dissolved silicate levels (Figure 5c) that inhibit diatom blooms [*Egge and Aksnes*, 1992]. This pattern agrees with an iron limitation scenario in SSW [see *Sedwick et al.*, 1999, and references therein] and with the suggestion that an initial iron limitation could force a secondary DSi limitation [*Hutchins and Bruland*, 1998]. Reduced primary productivity in oceanic SSW (due to an initial iron limitation) is consistent with near-equilibrium offshore pCO_2 levels (Figure 5a), which contrasted sharply with coastal waters that were extremely undersaturated in CO_2 and depleted in nitrate during this season (i.e., austral summer; Figures 6b and 6h). Consequently, the contrasting pCO_2 and nitrate levels between oceanic and coastal waters of Patagonia can be attributed to a rapid consumption of SSW macronutrients when this water enters the archipelago, with the consumption of oceanic macronutrients likely triggered by the inputs of dissolved iron (DFe) and DSi from the continent (e.g., freshwater inputs and the continental shelf). Because CO_2 undersaturation of surface waters was linked to low-salinity waters (Figure 4), we expect that the inputs of freshwater play a key role in determining air-sea CO_2 fluxes of Pacific Patagonia. The southern coast of Chile is characterized by a high discharge of freshwater into the southeastern Pacific Ocean [*Dávila et al.*, 2002]. At 50°S, very high levels of precipitation [*Dávila et al.*, 2002], in addition to the melting ice [*Rignot et al.*, 2003], can explain the austral summer surface salinity min-

ima off SPIF (Table 2), as well as the offshore surface salinity gradients [*Dávila et al.*, 2002, *Antezana*, 1999].

[39] The fjord and channels with year-round inputs of freshwater are expected to be permanently stratified and probably permanently CO_2-undersaturated (Figure 6b). The water column stratification derived from freshwater inputs is also a key factor that triggers phytoplankton blooms in nutrient-rich waters [e.g., *Smith and Nelson*, 1986; *Holmedal and Utnes*, 2006; *Ji et al.*, 2007, 2008]. These highly stratified surface waters act as an ample sink of CO_2 because of the high CO_2 solubility at these cold latitudes (Figures 11c and 11e) and the efficient reduction in the pCO_2 by photosynthesis (Figure 10; see section 3.4). We suggest that the portion of the coastal ocean near SPIF that remains stratified for most of the year has a particularly strong capacity to act as a sink for atmospheric CO_2, because of the interaction between physical, chemical, and biological factors, which can be collectively designated as the "alkalinity-stratification-biological pump" (ASBP); this concept is developed further in section 4.2.2.

4.2.2. Alkalinity-Stratification-Biological Pump

[40] High or moderate primary production rates measured in fjord surface waters during warm periods [e.g., *Pizarro et al.* 2000, 2005; *Iriarte et al.*, 2007; *González et al.* 2010] suggest that consumption of C_T by photosynthesis is the main factor driving the rapid depletion of pCO_2 in surface waters. Indeed, the highly productive and stratified surface waters in the fjords of Patagonia were particularly low in pCO_2 (e.g., Figures 8 and 9). Conversely, salty subpycnocline waters were supersaturated in CO_2 (Figure 9). This latter pattern confirms a high degree of vertical segregation between the autotrophic activity in the surface layer and the heterotrophic activity deeper in the water column, described by the GPP/CR ratio (Figure 9g). Additionally, while the input of C_T from deep to surface water is limited by a strong halocline, particulate organic carbon (POC) crosses the pycnocline during sedimentation events [*Iriarte et al.*, 2007], exporting organic carbon to more alkaline subpycnocline waters. The subsequent respiration of organic matter in subpycnocline waters is expected to be less efficient at increasing pCO_2 because of the higher buffer capacity of these saltier waters (see section 3.4).

[41] A strong halocline driven by large continental input of freshwater results in several biological, chemical, and physical phenomena that contribute to the ASBP: (1) most of the organic matter generated because of net primary productivity occurs in poorly buffered surface waters, which renders photosynthetic depletion of pCO_2 particularly efficient; (2) a portion of the organic matter that was generated in surface waters is respired in more highly buffered subpycnocline waters; and (3) surface layers are isolated from C_T-enriched subpycnocline waters by a strong pycnocline. This last point implies that the vertical flux of other dissolved nutrients (e.g., nitrate) to the upper layer is also limited, so the question is: where are the nutrients coming from to sustain this production and keep pCO_2 low? The most evident source of nutrients is the horizontal advection of oceanic SSW into the fjord system: Macronutrient-rich SSW can stimulate the productivity in the fjords and channels of Patagonia without producing CO_2 outgassing (i.e., nutrient-rich SSW water was slightly undersaturated in CO_2; Figures 5b and 5c). A very different situation occurs in the coastal upwelling ecosystem, where nutrient-rich upwelled waters are invariably and strongly supersaturated in CO_2 [*Torres and Ampuero*, 2009].

[42] Additionally, nutrient recycling may also play a role in maintaining low pCO_2. Although we do not have any direct assessment of the extent of nutrient recycling in the upper layer, we expect that recycled nitrogen allows decrements in C_T concentrations in surface waters even at very low dissolved inorganic nitrogen concentrations [e.g., *Sambrotto et al.*, 1993; *Banse*, 1994; *Geider and La Roche*, 2002; *Schartau et al.*, 2007]. This excess of lost C_T, termed carbon overconsumption by *Toggweiler* [1993], implies that the organic material exported from surface water is enriched in carbon [*Sambrotto et al.*, 1993]. Indeed, the C:N ratios of particulate organic matter during postbloom conditions were particularly high in the northeastern Atlantic Ocean [*Körtzinger et al.*, 2001]. In a postbloom condition, when nutrient acquisition limits biomass production but not photosynthesis, an excess of carbon is expected to be released as polysaccharide exudation followed by the formation of transparent exopolymer particles (TEP) [*Wood and Van Valen*, 1990; *Engel*, 2002; *Schartau et al.*, 2007]. Because CO_2 is the main source of DIC for phytoplankton photosynthesis in the ocean [*Raven and Johnston*, 1991], TEP production can be directly related to the CO_2 uptake during conditions of nutrient shortage [*Engel*, 2002]. This circumstance may explain the reduced pCO_2 levels observed in nitrate-depleted surface waters (note in Figure 6 that the nitrate-poor summer waters were associated with very low levels of surface water pCO_2).

[43] The oceanographic coastal setting reported here, characterized by the mixing between macronutrient rich SSW and DSi-DFe-rich freshwater, is expected to cause events of intense coastal photosynthesis (compared with oceanic conditions). Because the resulting increment in POC includes TEP carbon [*Schartau et al.*, 2007], a fraction of the biological consumption of C_T used during the new production of POC is decoupled from the algal growth (i.e., extracellular POC is produced [*Schartau et al.*, 2007]). Regardless of how carbon is partitioned after being incorporated by autotrophs, the exportation of POC to subpycnocline waters should result is a net drawdown of CO_2 and removal of carbon from surface waters. Therefore, we cannot discard the enhancing effect caused by "carbon overconsumption," particularly under nutrient shortage conditions (e.g., postbloom situation) as we previously discussed.

[44] Additionally, the input of freshwater to the coastal waters (ocean freshening) has been associated with earlier blooms and earlier nutrients depletion [*Ji et al.*, 2007, 2008]; thus, the marked ocean freshening of coastal waters near SPIF are expected to trigger early spring blooms, prolonging the postbloom period (e.g., characterized by low pCO_2). In a different way, relatively high pCO_2 levels (CO_2-supersaturation) observed in saltier surface waters of Patagonia imply that water column mixing (i.e., the erosion of the pycnocline) could be the key mechanism in explaining CO_2 outgassing (e.g., in the shallow inner archipelago of Chiloe and near the windy Golfo de Penas; Figure 1).

[45] In summary, we have labeled ASBP as the interaction of three factors: (1) water column stratification (main physical factor); (2) high GPP/CR ratio in the upper layer (main biological factor); and (3) high efficiency of pCO_2 reduction

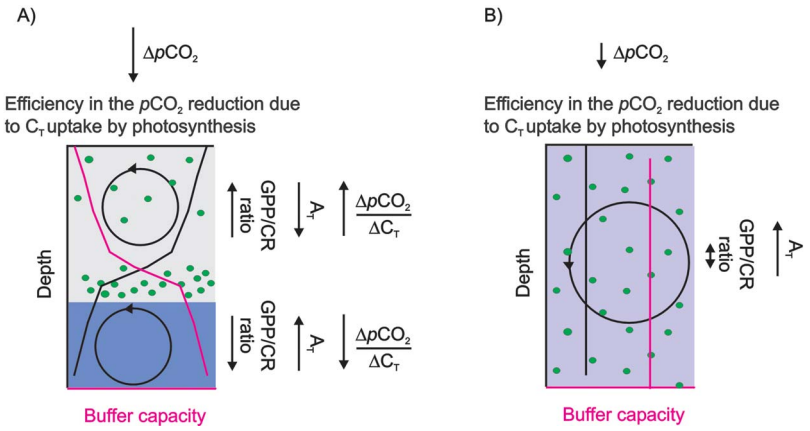

Figure 12. Representation of the linkages between water column stratification, CO_2 uptake by phytoplankton, and buffer capacity. (a) The ASBP concept as a highly stratified system in which the CO_2 flux (assumed to be proportional to the air-sea pCO_2 gradient) toward the upper layer is particularly intense due to the relatively high biological uptake and a low buffer capacity compared with a nonstratified water column (Figure 12b). (b) The reduction in surface water pCO_2 is lower because of the combined effect of the absence of vertical segregation between primary production and respiration, and the higher buffer capacity of the upper zone.

in terms of DIC and nutrient consumption (main chemical factor). A conceptual diagram of the ASBP is provided in Figure 12. We suggest that this interaction between physical, biological, and chemical factors explains the high CO_2 undersaturation levels in low-salinity surface waters (i.e., low buffer capacity and high GPP/CR ratio of surface water) and its persistence over time (i.e., continuous supply of nutrient-rich but pCO_2-low SSW, high efficiency in reduction surface water pCO_2, and probably carbon overconsumption).

[46] The "autotrophic behavior" of the estuarine systems of Patagonia described here is in contrast with the typical "heterotrophic behavior" of northern estuaries, which receive high inputs of organic matter [*Frankignoulle et al.*, 1998, and references therein]. This contrasting behavior may depict the fragility of the ASBP to any increment in organic matter content of the incoming freshwater, i.e., the asymmetric relationship between organic carbon production-remineralization and pCO_2 (shown in Figure 10a) can allow a fast shift in the direction of CO_2 flux.

4.2.3. Quantification of the CO_2 Sink in Fjords and Channels of Patagonia

[47] Data presented here strongly suggest that Patagonian fjords are a sink for atmospheric CO_2 during the austral summer period. The estimate of the intensity of CO_2 fluxes is subject to uncertainty, mainly associated with the estimation of k (piston velocity). The most important process controlling k is turbulence at the air-seawater interface, and because the wind stress on the surface ocean is the main generator of turbulence, k is usually parameterized as a function of wind speed. At low wind speeds, parameter estimation is complicated by the presence of surfactants, convective cooling, chemical enhancement, and other factors. In coastal systems, spatial and seasonal variations of gas transfer velocity are also mainly related to wind speed, but are also modulated by water current and bathymetry [*Borges et al.*, 2004]. Thus, the use of a generic relationship between gas transfer velocity and wind speed in estuaries carries significant uncertainty [*Borges et al.*, 2004].

[48] The magnitude of k reported here should be interpreted as a first approximation, and with particular caution, because onboard wind speed measurements could not necessarily represent the mean wind speed regimen in the fjords and channels of Patagonia. The estimated CO_2 flux in Patagonia (-5 mol C m^{-2} yr^{-1}) is particularly large compared with analogous studies on the Atlantic side of the Patagonian shelf (-1.6 mol C m^{-2} yr^{-1} [*Bianchi et al.*, 2005]). Indeed, mean CO_2 undersaturation reported here (-51 μatm) exceeds analogous estimations for the Atlantic Patagonia shelf (-24 μatm [*Bianchi et al.*, 2005]). We suggest that this difference may be due to the influence of high inputs of freshwater by orographycally enhanced precipitations along the western side of the southern cone of America. This "freshwater" factor may be critical for (1) the transport of continental nutrients (dissolved iron and silicic acid) that may enhance diatom productivity in a region influenced by oceanic SSW that lacks significant concentrations of those elements, and (2) the functioning of the "alkalinity-stratification-biological pump."

[49] Based on the CO_2 fluxes from Pacific Patagonian shelf water presented here and the estimates of the mean CO_2 flux of Atlantic Patagonian shelf waters (i.e., -1.6 mol C m^{-2} yr^{-1} [*Bianchi et al.* 2005]), we conclude that Patagonian coastal waters (a total area of 1.1×10^6 km^2) can absorb approximately 12.6×10^6 t C per warm season (3 and 9.6×10^6 t C per warm season for the Pacific and Atlantic sides, respectively), likely representing one of the largest coastal CO_2 sinks in the Southern Hemisphere.

[50] Although the estimation of mean CO_2 fluxes throughout the upwelling area of central and northern Chile was precluded by the paucity of data, we have made a very raw estimation of the maximum CO_2 outgassing, scaling a CO_2 flux of 3.5 mol m^{-2} yr^{-1} (associated with typical conditions of strong CO_2 supersaturation that can be observed in central and northern Chile [*Torres et al.*, 2002; *Friederich et al.*, 2008]) up to the entire area, which is CO_2 supersaturated (36°S–23°S) during the upwelling season (austral

spring and summer). Assuming that this CO_2 flux is constant and extends 35 km offshore (an area equivalent to 5×10^4 km^2), this "maximum CO_2 outgassing" would be $\sim 1 \times 10^6$ t C per warm season. This theoretical maximum figure for CO_2 outgassing off Chile is still well below the 3×10^6 t C sequestered by the Pacific Patagonian shelf over the warm season. We therefore suggest that the CO_2 sequestration in the Patagonia fjord region during spring-summer could exceed the CO_2 source produced by the coastal upwelling system off central northern Chile during the same period.

[51] **Acknowledgments.** This research was funded by FONDECYT 1060694-1090624-1070713, the Center for Oceanographic Research in the eastern South Pacific (FONDAP COPAS Center CONICYT grant 150100007), and the Humboldt-2009 project (Spanish Ministry of Science and Education, grant CTM2008-02497-E). We thank the Huinay Foundation for marine station laboratories and vessel facilities in the Comau Fjord, North Patagonia (this paper is contribution 50 for Huinay Foundation). Also we thank Fundación CEQUA for financial support for M/V *Chonos* cruises. R Torres was supported in part by a FONDAP COPAS postdoctoral fellowship and FONDECYT 1060694. We are grateful to Carina Lange and Captain Akamine and the crew of R/V *Mirai* for their help with sediment collection and water sampling during the MR03-K04 and MR08–06 cruises. This work was a part of the joint research on "paleoceanography, biogeochemistry and physical oceanography in the coastal area off Chile" between FONDAP COPAS Center and Japan Agency for Marine-Earth Science and Technology. We thank Taro Takahashi from the Lamont-Doherty Earth Observatory of Columbia University and Rik Wanninkhof at NOAA for providing surface CO_2 data. We thank CDIAC, GLODAP, Servicio Hidrográfico y Oceanográfico de la Armada de Chile, Servicio Meteorológico de la Armada, JGOFS-Chile Project for providing the meteo-hydrographical data. We also thank two anonymous reviewers for their valuable suggestions.

References

Antezana, T. (1999), Hydrographic features of Magellan and Fuegian inland passages and adjacent Subantarctic waters, *Sci. Mar.*, *6*, 23–34.

Atkinson, L. P., A. Valle-Levinson, D. Figueroa, R. De Pol-Holz, V. A. Gallardo, W. Schneider, J. L. Blanco, and M. Schmidt (2002), Oceanographic observations in Chilean coastal waters between Valdivia and Concepción, *J. Geophys. Res.*, *107*(C7), 3081, doi:10.1029/2001JC000991.

Banse, K. (1994), Uptake of inorganic carbon and nitrate by marine plankton and Redfield ratio, *Global Biogeochem. Cycles*, *8*(1), 81–84, doi:10.1029/93GB02865.

Bianchi, A. A., L. Bianucci, A. R. Piola, D. Ruiz Pino, I. Schloss, A. Poisson, and A. F. Balestrini (2005), Vertical stratification and air-sea CO_2 fluxes in the Patagonian shelf, *J. Geophys. Res.*, *110*, C07003, doi:10.1029/2004JC002488.

Borges, A. V., B. Delille, L. S. Schiettecatte, F. Gazeau, G. Abril, and M. Frankignoulle (2004), Gas transfer velocities of CO2 in three European estuaries (Randers Fjord, Scheldt and Thames), *Limnol. Oceanogr.*, *49*(5), 1630–1641, doi:10.4319/lo.2004.49.5.1630.

Borges, A. V., B. Delille, and M. Frankignoulle (2005), Budgeting sinks and sources of CO2 in the coastal ocean: Diversity of ecosystems counts, *Geophys. Res. Lett.*, *32*, L14601, doi:10.1029/2005GL023053.

Brandhorst, W. (1971), Condiciones oceanográficas estivales frente a la costa de Chile, *Rev. Biol. Mar.*, *14*, 45–84.

Broecker, W. S., T. Takahashi, H. J. Simpson, and T.-H. Peng (1979), Fate of fossil fuel carbon dioxide and the global carbon budget, *Science*, *206*, 409–418, doi:10.1126/science.206.4417.409.

Butorovic, N. (2003), Resumen meteorológico año 2003: Estación Jorge C. Schythe, *An. Inst. Patagonia*, *32*, 79–86.

Butorovic, N. (2005), Resumen meteorológico año 2004 estación "Jorge C. Schythe" (53°08′S; 70°53′W; 6M S.N.M.), *An. Inst. Patagonia*, *33*, 65–71.

Cai, W.-J., M. Dai, and Y. Wang (2006), Air-sea exchange of carbon dioxide in ocean margins: A province-based synthesis, *Geophys. Res. Lett.*, *33*, L12603, doi:10.1029/2006GL026219.

Chaigneau, A., and O. Pizarro (2005), Surface circulation and fronts of the South Pacific Ocean, east of 120°W, *Geophys. Res. Lett.*, *32*, L08605, doi:10.1029/2004GL022070.

Chavez, F. P., T. Takahashi, W. J. Cai, G. Friederich, B. Hales, R. Wanninkhof, and R. A. Feely (2007), Coastal Oceans, in *The First State of the Carbon Cycle Report (SOCCR)*, edited by A. W. King et al., pp. 149–156, NOAA, Natl. Clim. Data Cent., Asheville, N. C.

Chen, C. A., and A. V. Borges (2009), Reconciling opposing views on carbon cycling in the coastal ocean: Continental shelves as sinks and near-shore ecosystems as sources of atmospheric CO_2, *Deep Sea Res. Part II*, *56*, 578–590, doi:10.1016/j.dsr2.2009.01.001.

Dávila, P. M., D. Figueroa, and E. Müller (2002), Freshwater input into the coastal ocean and its relation with the salinity distribution off austral Chile (35–55°S), *Cont. Shelf Res.*, *22*, 521–534, doi:10.1016/S0278-4343(01)00072-3.

Devynck, J. L. (1971), *Precipitaciones diarias en Chile. Periodo: 1950–1969 y mapa pluviométrico de Chile. Promedio anual. Período 1931–1960*, Departamento de Geofísica, Universidad de Concepción, Chile.

Dickson, A. G., and C. Goyet (Eds.) (1994), Handbook of Methods for Analysis of the Various Parameters of the Carbon Dioxide System in Sea Water, *Rep. ORNL/CDIAC-74 C*, version 2, Dep. of Energy, Washington, D. C. (Available at http://cdiac.ornl.gov/oceans/DOE_94.pdf.)

Dickson, A. G., and F. J. Millero (1987), A comparison of the equilibrium constants for the dissociation of carbonic acid in seawater media, *Deep Sea Res.*, *34*, 1733–1743, doi:10.1016/0198-0149(87)90021-5.

Ducklow, H. W., and S. L. McCallister (2004), The biogeochemistry of carbon dioxide in the coastal oceans, in *The Sea*, vol. 13, *The Global Coastal Ocean: Multiscale Interdisciplinary Processes*, edited by R. Robinson, K. Brink, and B. J. Rothschild, pp. 269–315, Harvard Univ. Press, Cambridge, Mass.

Dugdale, R., J. Goering, R. Barber, R. Smith, and T. Packard (1977), Denitrification and hydrogen sulfide in the Peru upwelling region during 1976, *Deep Sea Res.*, *24*(6), 601–608, doi:10.1016/0146-6291(77)90530-6.

Egge, J. K., and D. L. Aksnes (1992), Silicate as regulating nutrient in phytoplankton competition, *Mar. Ecol. Prog. Ser.*, *83*, 281–289, doi:10.3354/meps083281.

Engel, A. (2002), Direct relationship between CO_2 uptake and transparent exopolymer particles production in natural phytoplankton, *J. Plankton Res.*, *24*, 49–53, doi:10.1093/plankt/24.1.49.

Fedele, A. (1993), Razón N-NO3-:P-PO4-anómala, un trazador químico para la masa de agua ecuatorial subsuperficial (AESS), thesis, 134 pp., Universidad Católica de Valparaíso.

Feely, R. A., C. L. Sabine, J. M. Hernandez-Ayon, D. Ianson, and B. Hales (2008), Evidence for upwelling of corrosive "acidified" water onto the continental shelf, *Science*, *320*, 1490–1492, doi:10.1126/science.1155676.

Figueroa, D., and C. Moffat (2000), On the influence of topography in the induction of coastal upwelling along the Chilean coast, *Geophys. Res. Lett.*, *27*, 3905–3908, doi:10.1029/1999GL011302.

Frangópulos, M., J. L. Blanco, M. Hamamé, S. Rosales, R. Torres, A. Valle-Levinson (2007) Análisis y diagnóstico de las principales características oceanográficas del área marina costera protegida Francisco Coloane, informe final, Proyecto GEF-PNUD, Punta Arenas, Chile.

Frankignoulle, M., G. Abril, A. Borges, I. Bourge, C. Canon, B. Delille, E. Libert, and J. M. Théate (1998), Carbon dioxide emissions from European estuaries, *Science*, *282*, 434–436, doi:10.1126/science.282.5388.434.

Friederich, G. E., J. Ledesma, O. Ulloa, and F. P. Chavez (2008), Air–sea carbon dioxide fluxes in the coastal southeastern tropical Pacific, *Prog. Oceanogr.*, *79*, 156–166, doi:10.1016/j.pocean.2008.10.001.

Fuenzalida, R., W. Shneider, J. Garcés-Vargas, L. Bravo, and C. Lange (2009), Vertical and horizontal extension of the oxygen minimum zone in the Eastern South Pacific Ocean, *Deep Sea Res. Part II*, *56*, 992–1003, doi:10.1016/j.dsr2.2008.11.001.

Gaiero, D. M., J. L. Probst, P. J. Depetris, S. M. Bidart, and L. Leleyter (2003), Iron and other transition metals in Patagonian riverborne and windborne materials: Geochemical control and transport to the southern South Atlantic Ocean, *Geochim. Cosmochim. Acta*, *67*(19), 3603–3623, doi:10.1016/S0016-7037(03)00211-4.

Garreaud, R., and R. Munoz (2005), The low-level jet off the subtropical west coast of South America: Structure and variability, *Mon. Weather Rev.*, *133*, 2246–2261, doi:10.1175/MWR2972.1.

Garreaud, R., J. Rutllant, and H. Fuenzalida (2002), Coastal lows in north-central Chile: Mean structure and evolution, *Mon. Weather Rev.*, *130*, 75–88, doi:10.1175/1520-0493(2002)130<0075:CLATSW>2.0.CO;2.

Geider, R. J., and J. La Roche (2002), Redfield revisited: Variability in the N:P ratio of phytoplankton and its biochemical basis, *Eur. J. Phycol.*, *37*, 1–17, doi:10.1017/S0967026201003456.

GLOBALVIEW-CO_2 (2009), Cooperative Atmospheric Data Integration Project - Carbon Dioxide, CD-ROM, NOAA ESRL, Boulder, Colo. (Also available on Internet via anonymous FTP to ftp.cmdl.noaa.gov, Path: Ccg/co2/GLOBALVIEW)

González, H. E., et al. (2010), Primary production and plankton dynamics in the Reloncaví Fjord and the Interior Sea of Chiloé, northern Patagonia, Chile, *Mar. Ecol. Prog. Ser.*, *402*, 13–30, doi:10.3354/meps08360.

Goyet, C., R. I. Goncalves, and F. Touratier (2009), Anthropogenic carbon distribution in the eastern South Pacific Ocean, *Biogeosciences*, *6*, 149–156, doi:10.5194/bg-6-149-2009.

Haraldsson, C., L.G. Anderson, M. Hassellöv, S. Hulth, and K. Olsson (1997), Rapid, high precision potentiometric titration of alkalinity in ocean and sediment pore waters, *Deep Sea Res, Part I*, *44*, 2031–2044, doi:10.1016/S0967-0637(97)00088-5.

Holmedal, L. E., and T. Utnes (2006), Physical–biological interactions and their effect on phytoplankton blooms in fjords and near-coastal waters, *J. Mar. Res.*, *64*, 97–122, doi:10.1357/002224006776412368.

Hutchins, L., and K. Bruland (1998), Iron-limited diatom growth and Si:N uptake ratios in a coastal upwelling regime, *Nature*, *393*, 561–564, doi:10.1038/31203.

Iriarte, J. L., H. González, K. Liu, C. Rivas, and C. Valenzuela (2007), Spatial and temporal variability of chlorophyll and primary productivity in surface waters of southern Chile (41.5–43°S), *Estuarine Coastal Shelf Sci.*, *74*(3), 471–480, doi:10.1016/j.ecss.2007.05.015.

Ji, R., C. Davis, C. Chen, D. Townsend, D. Mountain, and R. Beardsley (2007), Influence of ocean freshening on shelf phytoplankton dynamics, *Geophys. Res. Lett.*, *34*, L24607, doi:10.1029/2007GL032010.

Ji, R., C. Davis, C. Chen, D. Townsend, D. Mountain, and R. Beardsley (2008), Modeling the influence of low-salinity water inflow on winter-spring phytoplankton dynamics in the Nova Scotia Shelf–Gulf of Maine region, *J. Plankton Res.*, *30*(12), 1399–1416, doi:10.1093/plankt/fbn091.

Körtzinger, A., J. I. Hedges, and P. D. Quay (2001), Redfield ratios revisited: Removing the biasing effect of anthropogenic CO_2, *Limnol. Oceanogr.*, *46*, 964–970, doi:10.4319/lo.2001.46.4.0964.

Lefèvre, N., J. Aiken, J. Rutllant, G. Daneri, S. Lavender, and T. Smyth (2002), Observations of pCO_2 in the coastal upwelling off Chile: Spatial and temporal extrapolation using satellite data, *J. Geophys. Res.*, *107*(C6), 3055, doi:10.1029/2000JC000395.

Leth, O., and J. F. Middleton (2004), A mechanism for enhanced upwelling in central Chile: Eddy advection, *J. Geophys. Res.*, *109*, C12020, doi:10.1029/2003JC002129.

Lewis, E., and D. W. R. Wallace (1998), *Program Developed for CO_2 System Calculations. ORNL/CDIAC-105*. Carbon Dioxide Information Analysis Center, Oak Ridge National Laboratory, U. S. Dept. of Energy, Oak Ridge, Tenn.

Mehrbach, C., C. H. Culberson, J. E. Hawley, and R. M. Pytkowicz (1973), Measurement of the apparent dissociation constants of carbonic acid in seawater at atmospheric pressure, *Limnol. Oceanogr.*, *18*, 897–907, doi:10.4319/lo.1973.18.6.0897.

Paulmier, A., D. Ruiz-Pino, and V. Garcon (2008), The oxygen minimum zone (OMZ) off Chile as intense source of CO_2 and N_2O, *Cont. Shelf Res.*, *28*, 2746–2756, doi:10.1016/j.csr.2008.09.012.

Pizarro, O. (2000), Low frequency fluctuations in the eastern boundary current off South America: Remote and local forcing, Ph.D. thesis, Göteborg Univ., Gothenburg, Sweden.

Pizarro, G., J. L. Iriarte, V. Montecino, J. L. Blanco, and L. Guzmán (2000), Distribución de Biomasa Fitoplanctónica y productividad primaria máxima de Fiordos y Canales Australes en Octubre 1996, *Cienc. Tecnol. Mar*, *23*, 25–48.

Pizarro, G., V. Montecino, L. Guzmán, V. Muñoz, V. Chacón, H. Pacheco, M. Frangópulos, L. Retamal, and C. Alarcón (2005), Patrones locales recurrentes del fitoplancton en fiordos y canales australes (43°–56°) en primavera y verano, *Cienc. Tecnol. Mar*, *28*(2), 63–83.

Raven, J. A., and A. M. Johnston (1991), Mechanisms of inorganic-carbon acquisition in marine phytoplankton and their implications for the use of other resources, *Limnol. Oceanogr.*, *36*, 1701–1714, doi:10.4319/lo.1991.36.8.1701.

Rignot, E., A. Rivera, and G. Casassa (2003), Contribution of the Patagonia Icefields of South America to sea level rise, *Science*, *302*, 434–437, doi:10.1126/science.1087393.

Romero, O., and D. Hebbeln (2003), Biogenic silica and diatom thanatocoenosis in surface sediments below the Peru-Chile Current: Controlling mechanisms and relationship with productivity of surface waters, *Mar. Micropaleontol.*, *48*, 71–90, doi:10.1016/S0377-8398(02)00161-5.

Sambrotto, R. N., G. Savidge, C. Robinson, P. Boyd, T. Takahashi, D. M. Karl, C. Langdon, D. Chipman, J. Marra, and L. Codispoti (1993), Elevated consumption of carbon relative to nitrogen in the surface ocean, *Nature*, *363*, 248–250, doi:10.1038/363248a0.

Schartau, M., A. Engel, J. Schröter, S. Thoms, C. Völker, and D. Wolf-Gladrow (2007), Modelling carbon overconsumption and the formation of extracellular particulate organic carbon, *Biogeosciences*, *4*, 433–454, doi:10.5194/bg-4-433-2007.

Sedwick, P. N., G. R. Di Tullio, D. A. Hutchins, P. W. Boyd, F. B. Griffiths, A. C. Crossley, T. W. Trull, and B. Quéguiner (1999), Limitation of algal growth by iron deficiency in Australian Subantarctic region, *Geophys. Res. Lett.*, *26*, 2865–2868, doi:10.1029/1998GL002284.

Silva, N., and S. Neshyba (1979), On the southernmost extension of the Peru-Chile Undercurrent, *Deep Sea Res. Part A*, *26*, 1387–1393, doi:10.1016/0198-0149(79)90006-2.

Silva, N., N. Rojas, and A. Fedele (2009), Water masses in the Humboldt Current system: Properties, distribution, and the nitrate deficit as a chemical water mass tracer for Equatorial Subsurface Water off Chile, *Deep Sea Res. Part II*, *56*, 1004–1020, doi:10.1016/j.dsr2.2008.12.013.

Simpson, J. J., and A. Zirino (1980), Biological control of pH in the Peruvian coastal upwelling area, *Deep Sea Res. Part A*, *27*, 733–743, doi:10.1016/0198-0149(80)90025-4.

Smith, W. O., and D. M. Nelson (1986), Importance of ice edge phytoplankton production in the Southern Ocean, *BioScience*, *36*, 251–257, doi:10.2307/1310215.

Strickland, J. D. H. (1960), Measuring the production of marine phytoplankton, *Bull. Fish. Res. Board Can.*, *122*, 1–72.

Strub, T. P., J. M. Mesias, V. Montecino, J. Rutllant, and S. Salinas (1998), Coastal ocean circulation on western South America, in *The Sea*, vol. 11, edited by R. Robinson and K. H. Brink, pp. 273–314, John Wiley, New York.

Takahashi, T., et al. (2009), Climatological mean and decadal change in surface ocean pCO_2, and net sea-air CO_2 flux over the global oceans, *Deep Sea Res. Part II*, *56*, 554–577, doi:10.1016/j.dsr2.2008.12.009.

Thomas, H., Y. Bozec, K. Elkalay, and H. J. W. de Baar (2004), Enhanced open ocean storage of CO_2 from shelf sea pumping, *Science*, *304*, 1005–1008, doi:10.1126/science.1095491.

Toggweiler, J. (1993), Carbon overconsumption, *Nature*, *363*, 210–211, doi:10.1038/363210a0.

Torres, R. (2001), Carbon dioxide outgassing in coastal upwelling areas off northern and central Chile, Ph.D. thesis, Gothenburg Univ., Gothenburg, Sweden.

Torres, R., and P. Ampuero (2009), Strong CO_2 outgassing from high nutrient low chlorophyll coastal waters off central Chile (30°S): The role of dissolved iron, *Estuarine Coastal Shelf Sci.*, *83*, 126–132, doi:10.1016/j.ecss.2009.02.030.

Torres, R., D. Turner, N. Silva, and J. Rutllant (1999), High short-term variability of CO2 fluxes during an upwelling event off the Chilean coast at 30°S, *Deep Sea Res. Part I*, *46*, 1161–1179, doi:10.1016/S0967-0637(99)00003-5.

Torres, R., D. Turner, J. Rutllant, M. Sobarzo, T. Antezana, and H. González (2002), CO_2 outgassing off Central Chile (31–30°S) and northern Chile (24–23°S) during austral summer 1997: The effect of wind intensity on the upwelling and ventilation of CO_2-rich waters, *Deep Sea Res. Part I*, *49*, 1413–1429, doi:10.1016/S0967-0637(02)00034-1.

Torres, R., D. Turner, J. Rutllant, and N. Lefèvre (2003), Continued CO2 outgassing in an upwelling area off northern Chile during the development phase of El Niño 97–98 (July 1997), *J. Geophys. Res.*, *108*(C10), 3336, doi:10.1029/2000JC000569.

Wanninkhof, R. (1992), Relationship between wind speed and gas exchange over the ocean, *J. Geophys. Res.*, *97*, 7373–7382, doi:10.1029/92JC00188.

Wood, M. A., and L. M. Van Valen (1990), Paradox lost? On the release of energy-rich compounds by phytoplankton, *Mar. Microb. Food Webs*, *4*, 103–106.

G. Daneri and R. Torres, Centro de Investigación en Ecosistemas de la Patagonia, Universidad Austral de Chile, Bilbao 449, Coyhaique, Chile. (rtorres@ciep.cl)

C. M. Duarte and S. Rúiz-Halpern, Department of Global Change Research, IMEDEA, Instituto Mediterráneo de Estudios Avanzados, Miquel Marqués 21, 07190 Esporles, Mallorca, Spain.

M. Frangopulos, Centro de Estudios del Cuaternario (Fundación CEQUA), 21 de mayo 1690, Casilla 737, Punta Arenas, Chile.

M. Fukasawa and N. Harada, Research Institute for Global Change, Japan Agency for Marine-Earth Science and Technology Center, 2-15 Natsushima-cho, Yokosuka, 237-0061, Japan.

H. E. González, Instituto de Biología Marina, Universidad Austral de Chile, Casilla 567, Valdivia, Chile.

E. Mayol, Laboratorio Internacional de Cambio Global, CSIC-PUC, Facultad de Ciencias Biológicas, Pontificia Universidad Católica de Chile, Edificio 210, Of. 425, Ave. Bernardo O'Higgins 340 ó Portugal 49, Casilla 114-D, Santiago, Chile.

S. Pantoja, Centro de Investigación Oceanográfica en el Pacífico Sur Oriental, Universidad de Concepción, Casilla 160-C, Concepción, Chile.

J. A. Rutllant, Departamento de Geofísica, Facultad de Ciencias Físicas y Matemáticas, Universidad de Chile, Santiago, Chile.